Occurrence of polycyclic aromatic hydrocarbon (PAH) in soils around two typical lakes in the western Tian Shan Mountains (Kyrgyzstan, Central Asia): Local burden or global distillation?

Qianyu Li [a,c], Jinglu Wu [a,b,*], Jianchao Zhou [a], Kadyrbek Sakiev [d], Diana Hofmann [e]

[a] *State Key Laboratory of Lake Science and Environment Research, Nanjing Institute of Geography and Limnology, Chinese Academy of Sciences, Nanjing 210008, China*

[b] *Ecology and Environment of Central Asia, Chinese Academy of Sciences, Urumqi 830011, China*

[c] *University of Chinese Academy of Sciences, Beijing 100039, China*

[d] *Institute of Geology, National Academy of Sciences, Bishkek 720001, Kyrgyystan*

[e] *Institute of Bio- and Geosciences, IBG-3: Agrosphere, Forschungszentrum Jülich, Jülich 52425, Germany*

**Corresponding author:*

E-mail address: w.jinglu@niglas.ac.cn

Tel., +86-025-86882159

Abstract: The United Nations Educational, Scientific and Cultural Organization (UNESCO) world natural heritage Tian Shan Mountains, situated in Central Asia, have experienced a dramatic increase in polycyclic aromatic hydrocarbon (PAH) contamination, not only because of increasing volumes of tourism-derived traffic but also because of the atmospheric transport of polluted westerly winds under global distillation effect. To assess the significance of two possible sources of PAHs, 16 priority PAHs were determined in 39 soil samples collected in August 2013 around Lake Issyk-Kul (YKR, 1,606 m) and Lake Son-Kul (SKR, 3,010 m) as typical mountain lakes in the western Tian Shan Mountains. Total PAH concentrations ranged from 52 ng/g dw to 9439 ng/g dw. The highest PAH levels were found in the industrial and urban areas of the YKR (>1000 ng/g dw); however higher levels were in the agricultural and rural areas of two regions (300-1000 ng/g dw), both dominated by 4-,5-ringed PAHs. In contrast, the lowest PAH levels (<200 ng/g dw) were mostly distributed in the pristine areas, dominated by 3-,4-ringed PAHs. Diagnostic ratio and Positive Matrix Factorization model infer that high PAH levels were mainly generated by petroleum combustion derived from local burgeoning tourism traffic beside road construction, indicated by simultaneously measured *n*-alkanes features (low carbon preference index and pristane/phytane ratio close to 1 with high unresolved complex mixture values). On the contrary, low PAH levels primarily from biomass combustion with unburned petroleum processes are ascribed to exogenous atmospheric transport under global distillation effect, because *n*-alkane sources here are biogenic input without petroleum contamination. An altitudinal/temperature dependence of 2-,3- and

4-ringed PAHs was significant in the SKR, and the soils in the SKR serve as a “sink” for PAHs in global cycling.

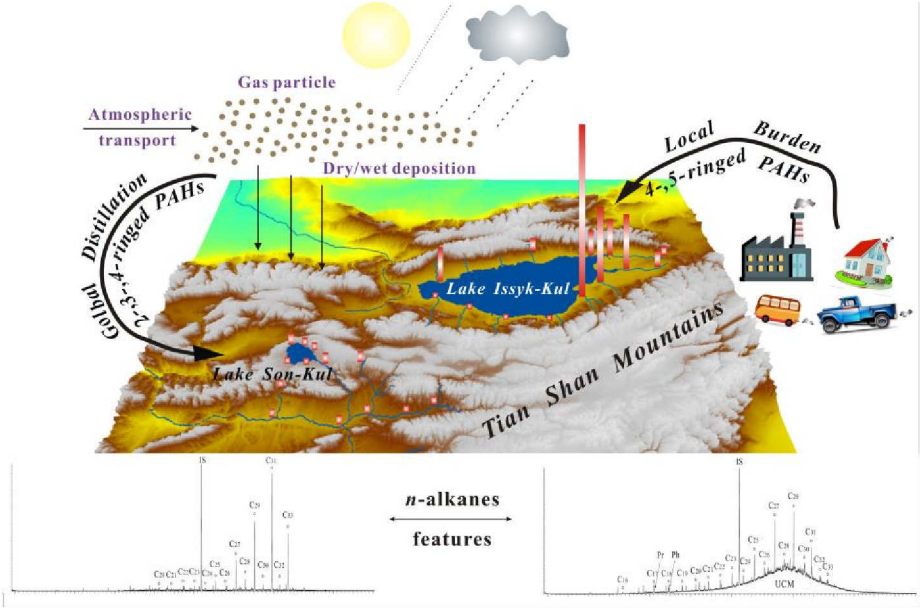

Keywords: soils, PAHs, *n*-alkanes, combustion, atmospheric transport, altitude

Highlights

- Three patterns of PAH distribution are clustered in soils around two mountain lakes.
- High PAH levels in the east of Lake Issyk-Kul region owe to petroleum combustion from tourism-derived traffic.
- Lake Son-Kul region serve as a “sink” for 2-,3-,4-ringed PAHs in global cycling.
- *N*-alkane features help to distinguish local PAH burden and global PAH distillation.

1. Introduction

The Tian Shan Mountains (40° ~ 45°N, 67° ~ 95°E) are the largest high mountain systems of Central Asia with an average altitude of 4,000 m above sea level (a.s.l.), located in the Asian hinterland. This region is thought to be pristine environment and supports numerous species of rare flora and fauna (Baumer, 2012; Zhang et al., 2015). In the past few years, the environment of the Tian Shan Mountains has been deteriorated as a result of intense human activitity, especially in the areas surrounding mountain lakes, where human populations concentrate (Schmidt, 2011). Increase of population and expansion of land-use including agriculture, industry and tourism are generating elevated local emissions of pollutants, affecting directly the environment of the lakes in the Tian Shan Mountains (Bekmamat et al.,2016; Li et al., 2019). Polycyclic aromatic hydrocarbons (PAHs), one of these major pollutants, are of great concern because they are toxic, persistent, and bioaccumulate in nature (Kannan et al., 2005; Zhou et al., 2018), which has been identified as a potential environmental problem in the Tian Shan Mountains (Shen et al., 2017).

As semi-volatile compounds, PAHs can also be transported from relatively warm source regions to cold high mountain regions, undergoing long range atmospheric transport and “global distillation” effect (Fernández and Grimalt, 2003; Khairy et al., 2016). Therefore, exogenous PAH deposition plays more and more a vital role in high mountain regions. The Tian Shan Mountains overstretch in east-west-direction approximately 2,500 km from, northwest China to Kazakhstan, Kyrgyzstan,

Uzbekistan and Tajikistan (Zhang et al., 2015). Hence, PAH emissions from neighboring industrializing countries might be atmospheric transported to the Tian Shan Mountains with the result that dry/wet deposition in mountain lake areas further aggravated or even exceeded the local environmental disturbance. So far, the interest in differentiation between endogenous and exogenous inputs of PAHs in high mountain regions has increased, because it could help not only in elucidating local PAH burdens but, more important, in understanding the mechanisms operating on a larger scale of PAH global distillation effect (Guzzella et al., 2016).

PAHs generally occur in crude oil or refined petroleum products and are also formed during the combustion of fossil fuels or other organic substances (Laflamme and Hites, 1978). Similar to PAHs, also other aliphatic hydrocarbons (AHs) such as *n*-alkanes have been widely recognized as homologous organic contaminants from petroleum-related contamination when they present no obvious predominance of even or odd-carbon number, evidenced by many investigations especially in the marine environment (Jafarabadi et al., 2017; Shirneshan et al., 2017). Hence, *n*-alkanes features such as a lack of predominance of even or odd-carbon number, ratios of C_{17}/pristane (Pr) and C_{18}/phytane (Ph), and an appearance of unresolved complex mixture (UCM) are characterized as one type of useful petroleum biomarkers (de Souza et al., 2011; Shirneshan et al., 2017). Because *n*-alkanes can be expected to be more bioavailable and less persistent than PAHs in the environment compartments, their long-range atmospheric transport is negligible and they are prone to be accumulated in original regions (Silva et al., 2012). In this study, therefore, *n*-alkanes

are innovated as a helpful indicator to distinguish endogenous PAH input especially from petroleum contamination in high mountain regions.

Hence, we analyzed PAHs in soils around two typical mountain lakes (Issyk-Kul and Son-Kul) at different altitudes in the western Tian Shan, Kyrgyzstan. Our general objectives were to (1) elucidate the current contamination level of PAHs in soils around mountain lakes, (2) address the spatial distribution of PAHs under consideration of the regional difference in socio-economic development, and (3) ascertain the input pathways and possible sources of PAHs by relating to *n*-alkanes features and predominantly meteorologic conditions for better differentiating the contributions from local burden and global distillation, respectively, in the Tian Shan Mountains.

2. Materials and methods

2.1. Study area

Lakes Issyk-Kul and Son-Kul are two major mountain lakes of the western Tian Shan in Kyrgyzstan (Fig. 1a and 1b). Lake Issyk-Kul with an altitude of 1,606 m a.s.l. is the largest mountain lake of the Tian Shan Mountains. Average air temperature above the lakes are 17°C in July and -7°C in January, while the temperature in the surrounding mountains is always around 10°C lower. They are dominated by prevailing westerly winds, accounting for 60% of the total wind (Klerkx and Imanackunov, 2002). Precipitation in the Issyk-Kul region occurs mostly in summer time and increases from west (115 mm/y) to east (600 mm/y) (Mamatkanov et al.,

2006). Around the Lake Issyk-Kul, grassland is the dominant terrestrial habitat in this region, while arid conditions prevail in the west and northwest. Agriculture is the primary land use in areas near the lake with 80% used for pasture (in the southwestern and southern shores), the rest for cultivation and built up mainly in the eastern part (ABD, 2009). The population is more dense in the east around Karakol, the capital of the Issyk-Kul region. Another important town, Balykchy, is located at the western end of Lake Issyk-Kul (Fig. 1d) as significant transport center (lake shipping, rail terminal international airport and road junction, too) e.g. passenger railway that begun direct services in 2018.

Lake Son-Kul located in the southwest of Issyk-Kul is the second largest lake in Kyrgyzstan with the higher altitude of 3,010 m a.s.l. and fills the central depression of a plateau between two generally east-west-trending mountain ranges (Fig. 1b). The climate here is also controlled by the mid-latitude westerlies (Kriegel et al., 2013). Mean annual temperature in the basin is -3.5 °C, with mean temperatures of 11 °C in July and −20 °C in January. Mean seasonal precipitation is 300-400 mm from April to October and 100-150 mm from November to March (Mathis et al., 2014; Pacton et al., 2015). The Lake Son-Kul is famous for summer (June-September) pasturing and tourism.

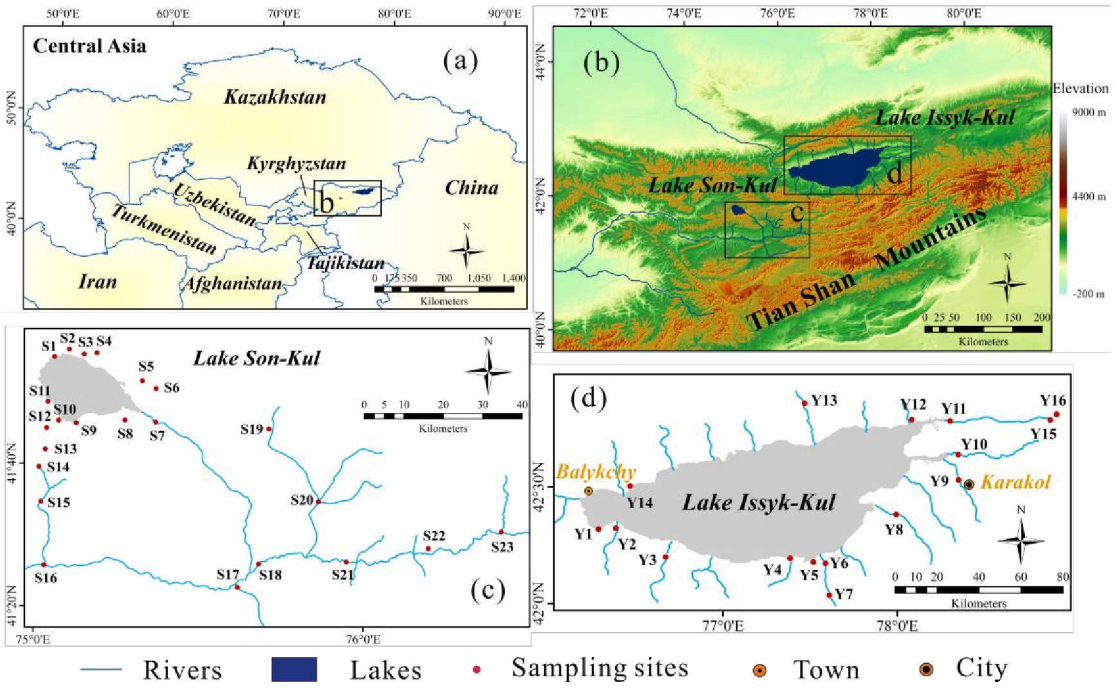

Fig. 1. Study area with sampling sites. (a) location (b) geomorphic map (c) sampling sites around Lake Son-Kul. (d) sampling sites around Lake Issyk-Kul.

2.2. Sample collection and preparation

Thirty-nine soil samples (0-5 cm) were collected around the two mountain lakes in August 2013 (Fig. 1c and 1d), of which 23 from the Son-Kul region (SKR, 41.37°N ~ 42.63°N, 75.02°E ~ 76.42°E) and 16 were from the Issyk-Kul region (YKR, 42.01°N ~ 42.83°N, 76.29°E ~ 78.97°E) (Table S1). Soil sampling points were selected about every 10–80 km depending on the topography and landscape conditions in the study area along the driving routes. To make the soil samples be representative, the following principles were applied: (a) the soil sampling sites should be more than 100 m away from highway, (b) located on the hilltop to avoid the alluvial soil when collecting samples in valleys, and (c) located on the sunny side of the mountain when collecting samples in the alpine areas. Soil samples were taken at intervals of 2 m

within a plot, and five or more samples were collected from each plot and mixed to represent a single, composite sample. A clean, stainless steel, 30-cm-diameter cylinder was used for sampling, and a Garmin 12 XL global positioning system (GPS) was employed to record the location of each sampling plot. Samples were wrapped in aluminum foil and sealed in clean polyethylene bags. As soon as possible, samples were stored at -20 ℃ before analysis.

All soil samples were freeze-dried and ground in an agate mortar to obtain 100 mesh (149 μm) powders for extraction. Five grams of homogenized soil sample were mixed with 3 g of anhydrous sodium sulfate (baked before at 550°C for 6 h) and extracted using dichloromethane using an accelerated solvent extraction (ASE) system (Dionex ASE-350, Sunnyvale, California). Freshly prepared copper granules were added to each sample to avoid potential interference of sulfur. The obtained extracts were further purified by a silica gel-alumina (2:1) column by sequential elutions first with 15 mL *n*-hexane (discarded), followed by 70 mL *n*-hexane/dichloromethane (7:3, v/v). The latter elution was then concentrated and treated according to Zhao et al. (2016).

2.3. Chemicals and reagents

Sixteen priority PAHs recommended by the EPA 610 method were purchased from Supelco (USA), including naphthalene (NaP), acenaphthylene (Acy), acenaphthene (Ace), fluorene (Flu), phenanthrene (Phe), anthracene (Ant), fluoranthene (Flt), pyrene (Pyr), benzo[*a*]anthracene (BaA), chrysene (Chr), benzo[*b*]fluoranthene (BbF), benzo[*k*]fluoranthene (BkF), benzo[*a*]pyrene (BaP),

dibenzo[*a,h*]anthracene (DahA), benzo[*g,h,i*]perylene (BghiP) and indeno[1,2,3-cd]pyrene (IP). Stock solutions of mixed standards were dissolved in dichloromethane/methanol (1:1, v/v) and stored in dark glass container at 4°C before use. All solvents (dichloromethane, methanol, n-hexane, acetonitrile) used for sample processing and analysis were chromatographic grade (Sinopharm Chemical Reagent Co. Ltd., Shanghai, China). Deionized water (Millipore Milli-Q system, MA, USA) was used throughout the analysis.

2.4. Instrument analysis

PAH determination was made using high-performance liquid chromatography (HPLC) instrument (Agilent 1200 HPLC, USA) equipped with a diode-array detector (DAD) and a series-wound fluorescence detector (FLD). The separation column was a Supelcosil LC-PAHs (ODS, 250 mm × 3.0 mm × 5 μm, Supelco, USA). Detailed instrumental conditions of the HPLC are referred to in Zhao et al., (2016).

2.5. Soil organic matter and *n*-alkane analyses

Total organic carbon (TOC) was analyzed with a EuroVecto5r EA3000 organic element analyzer (EuroVector S.R.L, Milan, Italy) after freeze-drying, pulverizing and treatment with 3 M HCl to remove carbonate of the samples. The *n*-alkane analysis was according to Zhang et al., (2016). Briefly, homogenized soil samples (three gram each) were Soxhlet extracted for 72 h with dichloromethane/methanol (9:1 v/v) after adding internal standard (*n*-tetracosane-d_{50}), and subsequently analyzed by GC–MS using an Agilent 7890A gas chromatograph, equipped with a DB–5MS

column (30 m × 0.25 mm × 0.25 μm) and an Agilent 5975 mass spectrometer.

2.6. Quality control and assurance

The qualitative analysis of PAHs is based on both UV spectra and the retention times of standard components, and the quantification was achieved using the external standard calibration curves. The calibration curves of individual compounds were established between the peak area and concentration of target compounds with the coefficients (*r*) ranging from 0.996 to 0.999. One standard solution of intermediate concentration was analyzed after every eight samples to recalibrate the retention time of the target compounds. Recovery of the spiked sample matrix ranged from 72% to 105% for the individual PAH compounds (Table S2). The method detection limits (MDLs) were determined as the concentration of analytes in a sample that yielded a peak signal-to-noise (S/N) ratio of 3 in the range of 0.03-1.42 ng/g dry weight, respectively. *n*-alkanes were identified via comparisons with reported mass spectra, interpretation of fragmentation patterns, and/or retention time. Quantification was made by an internal standard (n-tetracosane-d_{50}). For each set of samples, a procedural blank consisting of all reagents was run to check for cross contamination both PAH and *n*-alkane analyses. Results indicated that no carry-over was detected during the entire study.

2.7. Statistical analysis

The statistical analysis was performed using IBM Statistical Package for the Social Sciences (SPSS) version 22.0 (IBM, Armonk, NY) and Positive Matrix

Factorization（PMF) 5.0 receptor model released by the US EPA. A p-value <0.05 (two-tailed test) was used as a cut-off for statistical significance. Concentrations of PAHs and *n*-alkanes were expressed on a dry weight basis (ng/g dw for PAHs and μg/g dw for *n*-alkanes). For samples with concentrations below the MDLs, zero was assigned for statistical purposes, except in the PMF model. For the PMF model, if the concentration is less than or equal to the MDL, the original concentration should be substituted with half of the MDL, and the uncertainty (*Unc*) of these samples should be calculated by using equation: $Unc = 5/6 \times MDL$ (Norris et al., 2014).

3. Results

3.1. Concentrations and compositions of PAHs

The compositions of total 16 PAHs according ring number in soils from the SKR and YKR with their concentrations are illustrated in Fig. 2. PAHs were detected in all soil samples from the SKR with the total PAH concentrations from 54.5 to 428 ng/g dw. The highest PAH concentrations were found in the east part of Lake Son-Kul basin (S5-S7, S19) with 250-428 ng/g dw (mean 336 ng/g dw), whereas the lowest PAH concentrations were mainly appraised in the south of the SKR, with 54.5-120 ng/g dw (mean 97.6 ng/g dw). Among the PAHs, concentrations of low molecular weight (LMW) PAHs, including 2- and 3-ringed compounds, were 26.6-197 ng/g dw (mean 82.4 ng/g dw). As for high molecular weight (HMW) PAHs, concentrations of 4-ringed compounds were 17.4-187 ng/g dw (mean 59.7 ng/g dw), and finally, concentrations of 5- and 6-ringed compounds were 2.37-70.7 ng/g dw (mean 17.4

ng/g dw) and 4.07-50.3 ng/g dw (mean 18.0 ng/g dw), respectively. In general, the PAH compositions in the SKR are dominated by 3- and 4-ringed PAHs, attributing 27.5-63.2% (mean 45.1%) and 21.0-44.3% (mean 33.4%), respectively, of the total 16 PAHs. The differences in PAH composition patterns among various sampling sites were slight (Fig. 2).

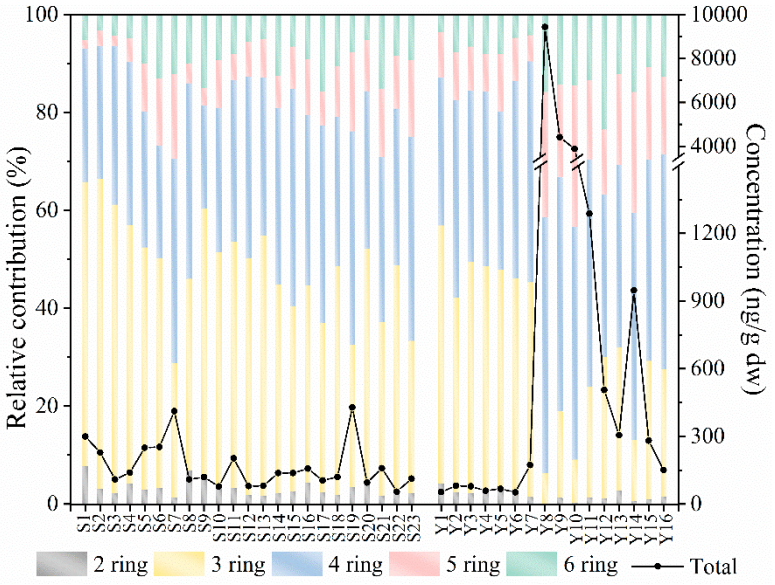

Fig. 2. Concentrations of total 16 PAHs summarized by ring number in soils from the SKR and YKR. (2 ring: NaP; 3 rings: the sum of Acy, Ace, Flu, Phe, and Ant; 4 rings: the sum of Flt, Pyr, BaA, and Chr; 5-rings: the sum of BbF, BkF, BaP, and DahA; 6-rings: the sum of BghiP and IP)

In contrast, in soils from the YKR the compositions of PAHs by ring number differ in dependence of sampling sites and the total PAH concentrations show an obvious upward trend from west starting from 51.9 ng/g dw to east with up to 9439 ng/g dw (Fig. 2). The highest PAH concentrations were appraised in the east and southeast shores of Lake Issyk-Kul (Y8-Y10), which were 3878-9439 ng/g dw (mean 5911 ng/g dw), whereas the lowest concentrations were observed in the south and

west, ranging from 51.9 ng/g dw to 81.2 ng/g dw (mean 65.3 ng/g dw). It is worth mentioning that the total PAH concentrations in site Y14 (on the western edge) with the high value of 947 ng/g dw is strongly contrasting to the most westerly sampling sites. Among the PAHs, concentrations of 2-, 3- and 4-ringed PAHs in the south and west part of the YKR were 1.46-2.44 ng/g dw (mean 1.89 ng/g dw) and 19.7-75.9 ng/g dw (mean 34.7 ng/g dw) and 16.1-78.0 ng/g dw (mean 31.7 ng/g dw), respectively. In contrast, 5- and 6-ringed PAHs show only minor values with 4.60-9.25 ng/g dw (mean 7.30 ng/g dw) and 1.90-7.26 ng/g dw (mean 5.14 ng/g dw), respectively. Therefore, PAH composition patterns are dominated by 3- and 4-ringed PAHs in the south and west part of the YKR, accounting for 29.2-52.7% (mean 43.2%) and 30.2-45.1% (mean 37.7%), respectively.

PAH composition patterns in the east and southeast part of the YKR, however, were significantly different. LMW PAHs occupied relatively lower, notably that the proportion of 3-ringed PAHs drastically decreased to 6.2-44.9% (mean 20.8%), in contrast to the percentages of HMW PAHs obviously increasing, of which 5-ringed PAHs attributed 2 times higher than that of the south and west sites, accounting for 11.8-28.9% (mean 21.9%) of the total 16 PAHs. The proportions of 4- and 6-ringed PAHs in the east and southeast part of the YKR both rose by 6%, accounting for 32.2-52.2% (mean 43.8%) and 8.05-15.8% (mean 13.2%), respectively. As result, PAH composition patterns in the east and southeast part of the YKR are predominated by 4-, 5- and 3-ringed PAHs.

Summing up, the concentrations and compositions of 16 PAHs did not varied

dramatically in the SKR as well as in the south and west part of the YKR, in conteast to the much higher concentrations in the east and southeast part of the YKR with PAH composition patterns significantly different from that of the other sites, which might indicate different sources of these PAHs.

4. Discussion

4.1. Spatial distribution and regional comparison

Numerous studies have shown that the soil matrix strongly retains PAHs. The partitioning concept of the soil sorption of organic contaminants implies that the sorption of hydrophobic organic molecules is determined by the organic matter (OM) content of the substrate (Tang et al., 2005). In the present study, the TOC contents of 39 soil samples ranged from 0.31 to 10.7% (Table S1). However, the results of our correlation tests, before and after the log transformations among individual and total PAHs with TOC showed that PAHs were not significantly correlated with TOC ($p > 0.05$), likely because PAHs and TOC had different sources and sorption processes. PAHs and other OMs that adhere to soil are in dynamic between adsorption and desorption. Vapor pressure of individual PAH determines the vapor-particle partitioning and thus the fraction that is available for long-range atmospheric transport and phase transfer into soil OM, so reaching equilibrium between PAHs and OMs is difficult (Bucheli et al., 2004; Yun et al., 2016). Another hypothesis might be that the soil PAH concentrations could not correlate well with TOC under the anthropogenic impact. It is well known that urban soils exhibit PAH concentrations much greater

than the contamination of soils in rural locations, reflecting the relationship between PAH loading and intensity of anthropogenic activities/population density (Wang et al., 2015).

According to the differences in PAH concentrations and compositions, the spatial distribution of PAHs in the study area was roughly classified into two parts; however, the reliability of the classification should be confirmed. Herein, to elucidate the distribution of PAHs and possible spatial association in the study area, a K-means cluster analysis was performed on the PAH concentrations and compositions across different sampling sites (Fig. 3). As result, sampling sites were clustered into three groups: Group 1 includes Y8-Y10 and Y14; Group 2 includes Y11-Y13, Y15-Y16, S7 and S19; and the remaining sampling sites were clustered into Group 3.

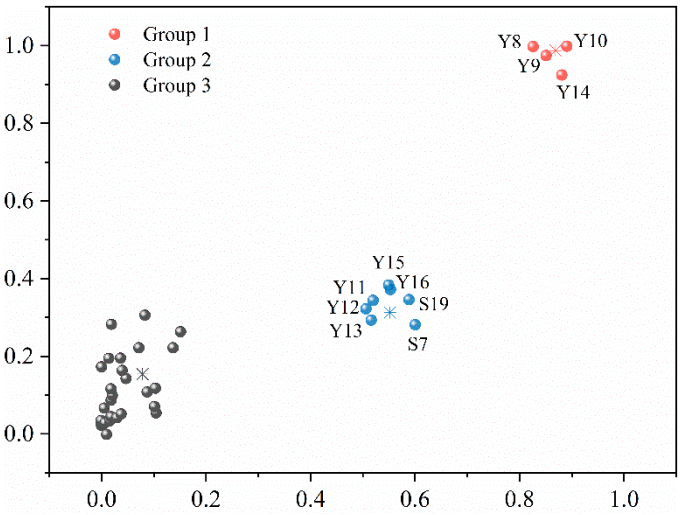

Fig. 3. K-means cluster analysis of 39 soil samples from the SKR and YKR. (Group 1 represents the industrial and urban areas of YKR. Group 2 represents the agricultural and rural areas of YKR and SKR. Group 3 represents mostly desert, grasslands, and alpine meadows.)

Sampling sites in Group 1 are generally located near the industrial and urban areas

of the YKR with the highest PAH levels at all (mainly >1000 ng/g dw). Y8 is near a dumping site close to a river where an abandoned Uranium mining site lies upstream. The Uranium mining factory gradually decayed after the collapse of the Soviet Union, and now it filled with slags and garbage (Tynybekov et al., 2008). Y9 and Y10 are close to Karakol, the largest city of the Lake Issyk-Kul region with about 93,000 residents - major tourist destination as well as industrial accumulation area of Kyrgyzstan. Similarly, Y14 is adjacent to Balykchy, the largest town of the Issyk-Kul region with a population of about 43,000 inhabitants. Earlier known as lake's fishing fleet, it is now a famous transportation hub with highways from the capital of Kyrgyzstan, Bishkek on the one side and splitting to Naryn and Karakol in the other direction, respectively. In 2018, a new railway began direct service connecting Kyrgyzstan, Uzbekistan and Kazakhstan (EurasiaNet, 2018). Therefore, intense industrial and urban activities, as well as frequent rail transport systems may be the reason for the high PAH levels, especially the HMW PAHs in Group 1. Compared to other industrial and urban areas around the world, PAH levels in Group 1 were slightly higher than, e.g. in Shanghai, China (Wu et al., 2018), Lanzhou, China (Jiang et al., 2016), Kocaeli, Turkey (Cetin et al., 2017), and Erbil, Iraq (Amjadian et al., 2016), and comparable to Dhanbad, India (Suman et al., 2016) and Rawalpindi, Pakistan (Saba et al., 2012), but significantly lower than the PAH levels in London, UK (Vane et al., 2014), Boston, USA (Wang et al., 2004) and the heavy industrial city of Delhi, India (Singh et al., 2012) (Table S3).

Sampling sites in Group 2 are close to villages, such as Grigorievka, Tyup (Y11)

and Kuturga (Y12), or nearby alpine regions (Y13, Y15, and Y16). These villages located on the northeastern shore of Lake Issyk-Kul where inhabitants cultivate land for farming and provide a high yield of cotton, fruits, and flowers (Baetov, 2003; ABD, 2009). Moreover, grasslands are also used for the construction of holiday houses and recreational camps, temporary canteens and food stands for tourists during the summer months, especially on the northern shore of the lake (Baetov, 2003; Schmidt, 2011). Thus, agricultural production practices probably contributed to the major release of PAHs there. Meanwhile, the nearby alpine regions are downstream in westerly wind direction of these villages, which semi-volatile PAH contaminants may efficiently transport to and cold condense into surrounding alpine regions. The similarity was also observed in sites S7 and S19 of the SKR. Overall, the PAH levels in Group 2 were mainly between 300-1000 ng/g dw, which is lower than many other agricultural and rural areas of the world (Table S3).

Group 3 covers remaining sampling sites in the study area. They basically maintain pristine environments where desert, grasslands, and alpine meadows cover much of the land. The PAH levels were low (mainly between 50-200 ng/g dw), suggesting that most of the study area has not been subject to substantial PAH contamination. Compared to PAH values from other remote mountain regions, PAH levels in Group 3 were lower than those in the southern side of the Himalaya (Devi et al., 2016), and mountains in southwestern China (Shi et al., 2014), similar to northern side of the Himalaya (Luo et al., 2016), the Changbai Mountains (Zhao et al., 2015) and mountains in western Canada (Choi et al., 2009), but higher than the PAH levels

found in the Alps (Tremolada et al., 2009), Tibetan Plateau (Zhou et al., 2018) and mountains in Tajikistan (Zhao et al., 2017) (Table S3).

4.2. Source apportionment

4.2.1. Diagnostic ratio and PMF model

PAHs emitted from different sources exhibit different molecular compositions; therefore, diagnostic ratios of selective individual compounds including Ant/(Ant + Phe), Flt/(Flt + Pyr), IP/(IP + BghiP) and BaP/BghiP are considered to be good indicators for identification of PAH sources (Yunker et al., 2002; Wu et al., 2018). Detailed description of such diagnostic ratios is provided in chapter S1 of the Supplementary material (SM). As shown in Fig. 4, the ratios of Ant/(Ant + Phe) > 0.1, 0.4 < Flt/(Flt + Pyr) < 0.5, 0.2 < IP/(IP + BghiP) < 0.5 and BaP/BghiP > 0.6 in Group 1 all suggested a predominant source of petroleum combustion, and most of them are from traffic emission. Group 2 was generally pointed on the ratio of Ant/(Ant+Phe) more than 0.1 and the traffic source typical ratio of BaP/BghiP almost higher than 0.6, too, but on ratios of Flt/(Flt + Pyr) and IP/(IP + BghiP) near to or more than 0.5, suggesting a mixture PAH sources from petroleum combined with coal, wood and/or grass combustion. In contrast, the ratio of Ant/(Ant + Phe) < 0.1 in Group 3, as well as ratios of Flt/(Flt + Pyr) and IP/(IP + BghiP) > 0.5 inferred a mixture of petrogenic and combustion processes, mostly related to non-traffic sources (BaP/BghiP < 0.6).

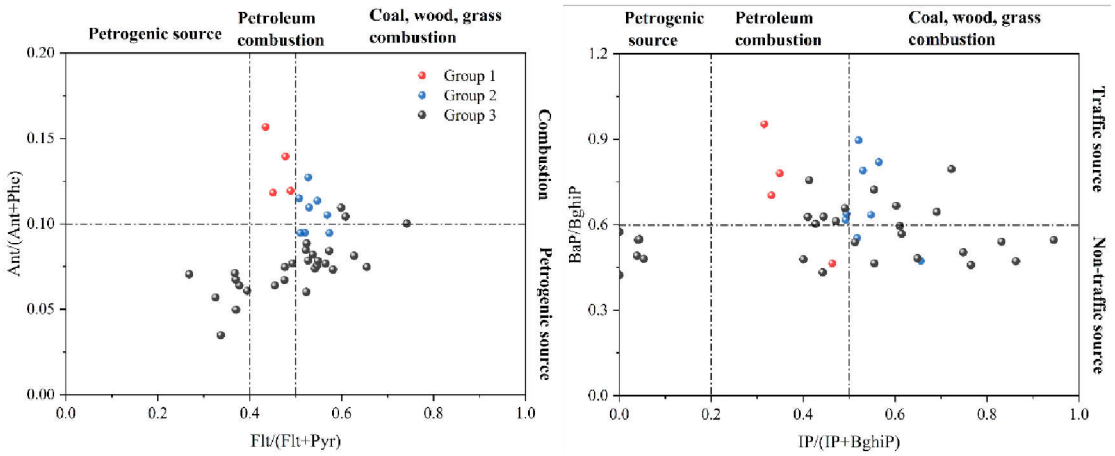

Fig. 4. Diagnostic ratio plots of Ant/(Ant+Phe) vs. Flt/(Flt+Pyr) and BaP/BghiP vs. IP/(IP+BghiP) in three groups of soil samples from the SKR and YKR.

To try to explore the major driving force further and to quantitatively assess the possible contributions of various sources with regard to PAH contamination, we adopted PMF to model the data of PAHs associated with the soils in the study area. The detailed discripition of PMF analysis with PAH concentrations as input data including their limitation were presented in chapter S2 of the SM. Finally, three factors for Group 1, four factors for Group 2 and three factors for Group 3 were selected for further discussion in this study (Fig. S1). The PMF pattern of Group 1 for Factors 1 and 2 are both heavily weighted in the vehicular-like compounds BghiP, BaP, BbF, BkF, IP, Flt, and Pyr. However, Factor 1 is enriched in BghiP and BaP relative to Factor 2, indicating that Factor 1 might be gasoline-powered whereas Factor 2 is more similar to a diesel-like vehicle profile (Khalili et al., 1995; Ravindra et al., 2006). Moreover, Factor 3 is dominated by Phe, BaA, Flt Chr, IP, and BbF. These compounds are essential tracers from the emission of some types of coal combustion (Kannan et al., 2005) (Fig. S1a). As result by the PMF model, identified and quant PAH sources in Group 1 count to 20% to gasoline combustion, 56% to diesel combustion, and 24%

to coal combustion (Fig. 5).

The PMF pattern of Group 2 for Factor 1 and Factor 3 are also identified as gasoline and diesel-powered engine emissions, respectively, characterized by BghiP, DahA, and IP. Factor 2 of Group 2 with significant levels of BaA, Phe, BbF, and Chr is identified as coal combustion. Moreover, Factor 4 of Group 2 is predominately loaded on LMW PAHs (Phe, Flu, Acy, Ace) as well as Flt and Pyr. The predominance of LMW PAHs is usually from the petrogenic/petroleum processes. Acy and Flu have been reported also to be markers of wood/firewood combustion (Khalili et al., 1995). Thus, Factor 4 reflected the contributions of incomplete biomass combustion together with petrogenic/petroleum processes (unburned petroleum) (Fig. S1b). The quantitative contributions of these four PAH sources in Group 2 suggested that petroleum (gasoline and diesel) and coal combustion were both main driving force (48% and 34% of the total contribution, respectively), while PAH input from biomass combustion with petrogenic/petroleum processes was little, only accounting for 18% (Fig. 5).

The PMF pattern of Group 3 for Factor 1 had a heavy loading of LMW PAHs, which is also identified as biomass combustion together with petrogenic/petroleum processes. However, it was the main input of PAHs in Group 3, attributing 60% of the total contribution. Factor 2 of Group 3 is dominated by vehicular-like compounds BghiP, BaP, BbF, BkF, DahA but only accounted for 13%. In addition, Factor 3 of Group 3 with significant levels of Phe, Flt, Pyr, BaA and Ace is typically regarded as some types of coal combustion (27% of the total contribution) (Fig. S1c and Fig. 5).

Although the accuracy of quantitative contributions modeled by PMF may be insufficient, the dominant driving force of each component can be more clearly identified. Overall, the primary sources of PAHs in the study area were derived from gasoline and diesel combustion, some types of coal combustion and incomplete biomass combustion with petrogenic/petroleum processes. Gasoline and especially diesel combustion from vehicular emission is the predominant PAH source of Group 1 in the industrial and urban areas of the YKR. Mixed PAH sources from coal and petroleum (gasoline and diesel) combustion are both the main input in the agricultural and rural areas of the YKR and SKR (Group 2), whereas PAH sources in group 3 are generally dominated by biomass combustion with petrogenic/petroleum processes.

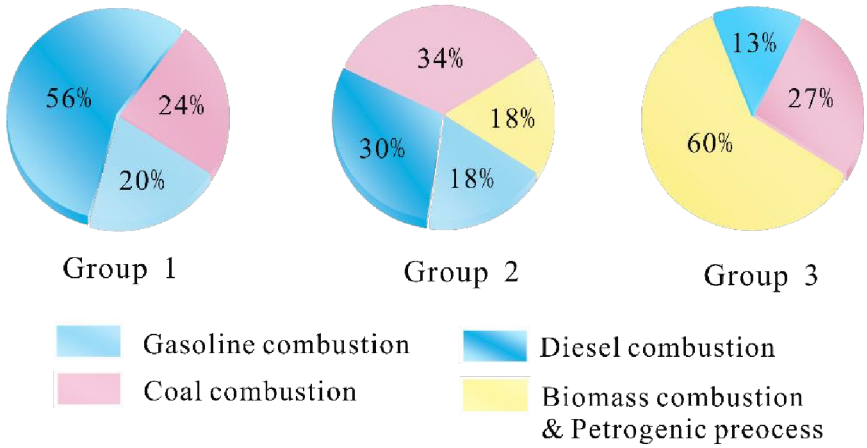

Fig. 5. Quantitative contributions of the identified sources by the PMF model in three groups of soil samples from the SKR and YKR.

4.2.2. Evidence for the local burden

As mentioned above, petroleum contamination contributed a large amount of PAH contaminant whether they were from combustion or non-combustion sources in the study area. However, there is no sub-division to distinguish these petroleum-derived

PAHs towards endogenous local activities or exogenous neighboring countries via atmospheric transport. Fortunately, *n*-alkanes, as homologous petroleum-related hydrocarbon contaminants, are less atmospheric transported from long distances, prone to accumulate in original regions (Silva et al., 2012). Hence, *n*-alkanes are introduced as second substance group to better identify endogenous petroleum contamination in the mountain regions. In this study, a set of 20 different *n*-alkanes between *n*-C16 and *n*-C35, associated with Carbon preference indexes (CPIs), UCMs, and isoprenoid ratios in the investigated soils among the three groups are demonstrated in Fig. 6. Base informations about using CPI, UCM and isoprenoid ratio for more detailed source apportionment were discussed in chapter S3 (SM).

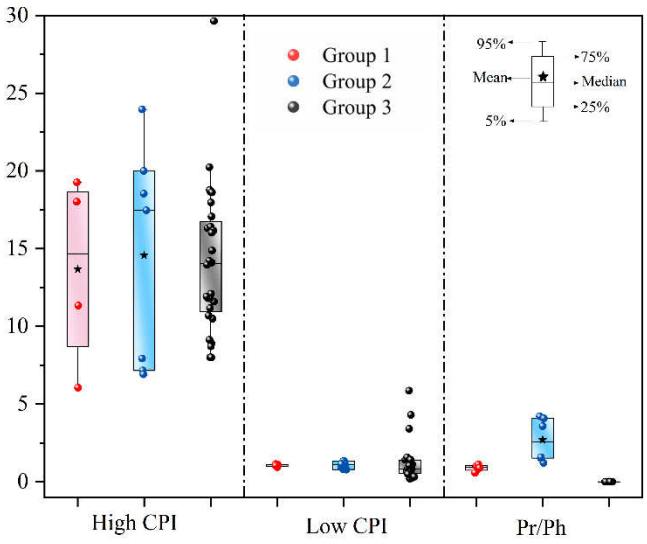

Fig. 6. Indices and ratios of *n*-alkanes in three groups of soil samples from the SKR and YKR (High CPI= 0.5*[(∑Odds C_{25}-C_{35})/ ∑Even C_{24}-C_{34}) + (∑Odds C_{25}-C_{35})/ ∑Even C_{26}-C_{36})]; Low CPI=0.5*[(∑Odds C_{17}-C_{23})/ ∑Even C_{16}-C_{22}) + (∑Odds C_{17}-C_{23})/ ∑Even C_{18}-C_{24})]).

The *n*-alkane distribution pattern of Group 1 exhibited no apparent odd to even

predominance of short-chain *n*-alkanes between *n*-C_{16} and *n*-C_{24} with overall low CPI values ranging from 0.94 to 1.14 (mean 1.05±0.09), but an odd to even predominance of long-chain *n*-alkanes (between *n*-C_{25} and *n*-C_{33}, C_{max} at *n*-C_{27} and *n*-C_{29}) with high CPI values ranging from 6.05-19.3 (mean13.7) (Fig. S2a and Fig. 6). Furthermore, high UCM concentrations (9.33-187 μg/g dw) in the range of *n*-C_{18}–*n*-C_{33} *n*-alkanes were observed in all soils in Group 1, and the UCM values showed a strong positive correlation with HMW PAH levels ($r = 0.82$, $p < 0.01$). Finally, the presence of Pr and Ph was an easy to find with the Pr/Ph ratio varying from 0.58-1.12. Together, all of these indicators suggested the contribution of local petroleum emissions from vehicular traffic and were also most likely associated with the oil transport and spillages (Simoneit, 1989; Jafarabadi et al., 2017). Besides, the strong odd-to-even carbon preference in the long chain *n*-alkanes reflected an additional biogenic input of high terrestrial plant, too (Zhang et al., 2016).

The *n*-alkane distribution pattern of Group 2 was similar to that of Group 1, except relatively low UCM values (5.13-92.9 μg/g dw) and changed Pr/Ph ratio varying from 1.21-4.21 (mean 2.34) (Fig.6). This is an indication that the *n*-alkanes loadings were affected both, by petroleum pollution and to some extent by coal burning.

However, the *n*-alkane distribution pattern of Group 3 presented two different types (Fig. S2b, c). The first unimodal distribution was found in the majority of the soil samples in Group 3, and contained an *n*-alkane distribution of a dominant odd long-chain with C_{max} at *n*-C_{31}, interpreted by overwhelming terrestrial high plant input

(Fig. S2b). The second bimodal distribution was observed in soils from Naryn River with an even short-chain dominance (C_{max} at *n*-C_{18} and *n*-C_{20}) together with an odd long-chain dominance (C_{max} at *n*-C_{29}, Fig. S2c), correlating to *n*-alkanes inputs for both bacterial activities and high plant lipids (Resmi et al., 2016; Jafarabadi et al., 2017). Different to the first two groups, UCM, Pr, and Ph were hardly found in soil samples from Group 3. Therefore, the biogenic *n*-alkanes input (without remarkable petroleum comtamination) is dominant in Group 3.

Concerning this fact, the origin of PAHs in Groups 1 and 2 was confirmed to be generally induced by endogenous petroleum-related activities, strongly evidenced by simultaneously *n*-alkane sources. Meanwhile, these petroleum-related activities corresponded well to local social-economic structures: in the industrial and urban areas of the YKR, petroleum-using activities related to the burgeoning tourist industry and road construction (Mikkola, 2012; EurasiaNet, 2018). Jenish (2017) has reported that the number of incorporated tourism firms rose by 22% from 154 in 2011 to 188 in 2015. About 73% of tour operators and travel agencies are based in the Issyk-Kul regional capital Karakol, followed by 10% in the Choplon Ata, which are both commercialized for tourism or built up for industry. The number of international vistors is expected to exceed 1 million persons per year, benefitting from local improved infrastructure and road/aviation safty (Mikkola, 2012; Djakypova, 2018). These both, burgeoning tourism and road rehabilitation have sparked the development of Issyk-Kul region, but, of course, resulted in the excessive local PAH burden. In the rural areas of the YKR and SKR, petroleum-related activities were confirmed by

agricultural and domestic activities, including the burning of fossil fuels to cook and heat (Baetov, 2003; Schmidt, 2011). However, in the most pristine environments of the study area, PAH sources are proved to be from biomass combustion with petroleum processes, but *n*-alkane sources disclosed no endogenous petroleum-related contamination here. Hence, the origin of PAHs in this region must be ascribable to exogenous input, such as atmospheric transport under the global distillation effect.

4.2.3. Contribution in global cycling

The global distillation effect is known as some organic pollutants move through the atmosphere from relatively warm source regions and condense at colder, higher latitudes/altitudes onto vegetation, soil and water bodies (Blais et al., 1998). It is based on physico-chemical properties of such organic pollutants and the climatic conditions. In the present study, 2-, 3- and 4-ringed PAHs are shown to be enriched at greater altitude/colder temperature, more than 5- and 6-ringed PAHs (Fig. 7a). The results suggested a positive correlation between 2-, 3- and 4-ringed PAHs and altitude ($r = 0.51\sim0.72$, $p < 0.05$, $n=28$) and a negative correlation between 2-, 3- and 4-ringed PAHs and temperature ($r = -0.69\sim-0.52$, $p < 0.05$, $n=28$). 5- and 6-ringed PAHs, however, displayed neither significant correlation with altitude ($r = -0.14\sim0.37$, $p > 0.05$, $n=28$), nor with temperature ($r = -0.13\sim0.21$, $p > 0.05$, $n=28$). This might be related to different vapor pressures of individual PAH compounds that 2-, 3- and 4-ringed PAHs (e.g. Nap, Acy, Phe) with overall higher vapor pressures are more volatile, expecting to be effectively distilled and transported, while 5- and 6-ringed

PAHs tend to remain near the source regions. Our findings in this study are consistent with the investigations of Miguel et al., (2004) and Luo et al., (2016). In addition, 2-, 3- and 4-ringed PAHs in Group 3 also showed a weak correlation with 5- and 6-ringed PAHs, inferring that their sources might be originated from different regions (Fig. 7a). As illustrated in Fig. 7b, 5- and 6-ringed PAHs in the south and west part of the YKR (part of Group 3) had a negative correlation with 5- and 6-ringed PAHs in the east part of the YKR (Group 1 and Group 2) ($r = -0.43$~-0.79, $p < 0.05$, n=16), suggesting the little influence of 5- and 6-ringed PAHs from local transportation by atmosphere across the YKR. Whereas, no correlation between 2-, 3- and 4-ringed PAHs in whole Group 3 and those in Group 1 and 2 ($r = -0.38$~0.35, $p > 0.05$, n=39) (Fig.7b, c) reveal that 2-, 3- and 4-ringed PAHs in the pristine environment of the study area should be generally from relatively remote regions under global transportation.

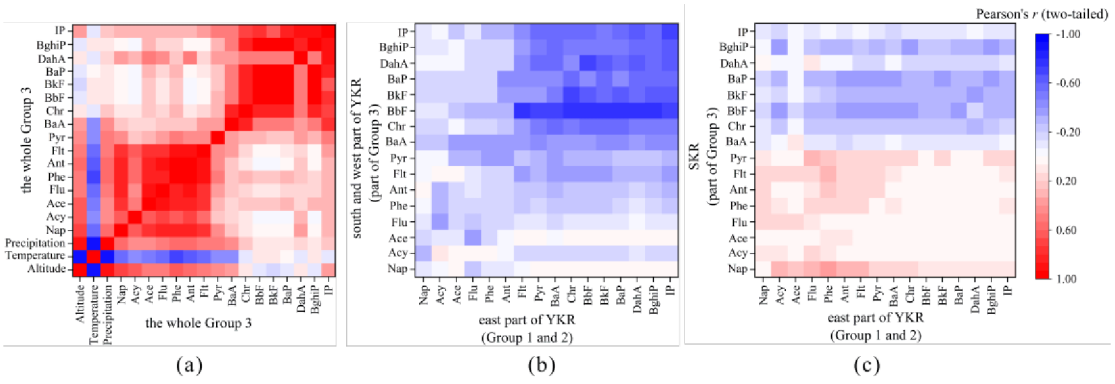

Fig. 7. Correlation coefficient (a) among individual PAH compounds and regional climatic conditions (altitude, temperature, precipitation) in whole Group 3; (b) between individual PAH compounds in the south and west part of YKR (part of Group 3) and those in the east part of YKR (Group 1 and 2); (c) between individual PAH compounds in the SKR (part of Group 3) and those in the east part of YKR (Group 1 and 2)

PAHs were suggested to be able to travel over moderate distances from source regions, whereby atmospheric particles are the main transport media allowing PAH deposition and accumulation in remote mountain regions including lakes and soils (Fernández and Grimalt, 2003). In this study, the proper transport distance of PAH through the atmosphere under global transportation was primary from westerly neighboring countries because the weather here is controlled by the mid-latitude westerlies (Wu et al., 2019). Ambient air monitoring activities in central Asia countries of former Soviet Union and Eastern Europe carried out by the Czech Hydrometeorological Institute from 2006 to 2008 reported the continuous air contamination with persistent PAHs not only in Kyrgyzstan (~20 μg/filter), but in Kazakhstan (~30 μg/filter) and even in relatively remote countries such as Romania, where the highest median PAH concentrations was measured (~100 μg/filter) (Pribylova et al., 2012). Consequently, under the prevailing westerly circulation and global distillation effect, exogenous polluted westerly winds transported long range especially 2-, 3- and 4-ringed PAHs pass country borders and finally deposited them to the SKR and YKR of Tian Shan Mountains.

Additionally, relatively higher concentrations of 2-, 3- and 4-ringed PAHs observed in the SKR than those in the south and west part of the YKR illustrate a slight downtrend from west to east, inferring that atmospheric transport of 2-, 3- and 4-ringed PAHs from the former Soviet Union countries with subsequently wet/dry deposition in the SKR is a result of temperature/altitudinal dependence. Reasonably, the soils in the SKR containing also 2-, 3- and 4-ringed PAHs chiefly serve as a

"sink" in global cycling.

5. Conclusions

This study provided comprehensive information on the priority hazard PAH occurrence in soils around two mountain lakes (YKR and SKR) at different altitudes of Tian Shan, Kyrgyzstan with their levels, spatial distributions, and source apportionments. According to the regional differences in socio-economic development, PAH contamination patterns in the study area are divided into three clusters. In the industrial and urban areas of the YKR were found the highest PAH levels (> 1000 ng/g dw), primarily ascribed to intensified petroleum combustion from vehicle. In the agricultural and rural areas of two regions, by contrast, higher PAH levels (300-1000 ng/g dw) were observed owing to mixed sources of coal and petroleum combustion. These two clusters result mainly from endogenous PAH input confirmed by several *n*-alkane features, which includes the presence of UCM, Pr, Ph, and low CPI close to 1. All results on the study of clusters in Group 1 and Group 2 corresponded well with local petroleum-related activities including burgeoning tourism along with frequently vehicular traffic and domestic cooking/heating. However, the lowest PAH levels distributed in the pristine environments of the study area were generally the result of exogenous source derived from westerly neighboring former Soviet Union countries through atmospheric transport under the global distillation effect. In detail, 2-, 3- and 4-ringed PAHs are prone to distill and enrich at colder climate/ higher altitude such as in the SKR, and the soils in the SKR chiefly

serve as a “sink” for PAHs in global cycling.

Acknowledgements

We thank the CAS Research Center for Ecology and Environment of Central Asia for assistance with this work. The authors thank Haiao Zeng and Long Ma for their field assistance. The paper was supported by the Strategic Priority Research Program of Chinese Academy of Sciences, Pan-Third Pole Environment Study for a Green Silk Road (XDA2006030101) and the National Natural Science Foundation of China (41671200; U1603242).

Reference

ADB, 2009. Issyk-Kul sustainable development project, Kyrgyz Republic. Volume 5: Strategic environmental management plan. Available online at https://www.adb.org/sites/default/files/project-document/62284/41548-kgz-dpta-v5-semp.pdf (Accessed on 21 May 2009)

Amjadian, K., Sacchi, E., Mehr, M.R., 2016. Heavy metals (HMs) and polycyclic aromatic hydrocarbons (PAHs) in soils of different land uses in Erbil metropolis, Kurdistan region, Iraq. Environ. Monit. Assess. 188(11), 605.

Baetov, R., 2003. Management of the Issyk-Kul basin. Mimeo. pp 22.

Baumer C (2012) The history of Central Asia: the age of the steppe warriors. I.B. Tauris, New York.Blais, J.M., Schindler, D.W., Muir, D.C.G., Donald, D.B., Rosenberg, B., 1998. Accumulation of persistent organochlorines in mountains of

western Canada. Nature 395, 585-588.

Bucheli, T.D., Blum, F., Desaules, A., Gustafsson, O., 2004. Polycyclic aromatic hydrocarbons, black carbon, and molecular markers in soils of Switzerland, Chemosphere 56(11), 1061-1076.

Cetin, B., Yurdakul, S., Keles, M., Celik, I., Ozturk, F., Dogan, C., 2017. Atmospheric concentrations, distributions and air-soil exchange tendencies of PAHs and PCBs in a heavily industrialized area in Kocaeli, Turkey. Chemosphere 183, 69-79.

Choi, S.D., Shunthirasingham, C., Daly, G.L., Xiao, H., Lei, Y.D., Wania, F., 2009. Levels of polycyclic aromatic hydrocarbons in Canadian mountain air and soil are controlled by proximity to roads. Environ. Pollut. 157(12), 3199-3206.

De Souza, A.R., Zago, M., Pollock, S.J., Sime, P.J., Phipps, R.P., Baglole, C.J., 2011. Genetic ablation of the aryl hydrocarbon receptor causes cigarette smoke-induced mitochondrial dysfunction and apoptosis. J. Biol. Chem. 286, 43214-43228.

Devi, N.L., Yadav, I.C., Qi, S.H., Yang, D., Gan, Z., Raha, P., 2016. Environmental carcinogenic polycyclic aromatic hydrocarbons in soil from Himalayas, India: implications for spatial distribution, sources apportionment and risk assessment. Chemosphere 144, 493-502.

EurasiaNet, 2018. Uzbekistan Opens New Railway Routes to Kyrgyzstan, Russia. Available online at https://eurasianet.org/uzbekistan-opens-new-railway-routes-to-kyrgyzstan-russia (Accessed on 22 March 2018).

Djakypova J, 2018. Kyrgyz Republic to Increase Regional Connectivity and Boost

Tourism in Prime Visitor Area, with World Bank Support. Available online at https://www.worldbank.org/en/news/press-release/2018/10/09/kyrgyz-republic-to-increase-regional-connectivity-and-boost-tourism-in-its-prime-traveler-attraction-area-with-world-bank-support (Accessed on 9 October 2018).

Fernández, P., Grimalt, J.O., 2003. On the global distribution of persistent organic pollutants. CHIMIA International Journal for Chemistry, 57(9), 514-521.

Grimalt, J.O., Drooge, B.L.V., Ribes, A., Fernández, P., Appleby, P., 2004. Polycyclic aromatic hydrocarbon composition in soils and sediments of high altitude lakes. Environ. Pollut. 131(1), 13-24.

Gogou, A., Bouloubassi, I., Stephanou, E.G., 2000. Marine organic geochemistry of the Eastern Mediterranean: 1. Aliphatic and polyaromatic hydrocarbons in Cretan Sea surficial sediments. Mar. Chem. 68, 265-282.

Guzzella, L., Salerno, F., Freppaz, M., Roscioli, C., Pisanello, F., Poma, G., 2016. POP and PAH contamination in the southern slopes of mt. Everest (Himalaya, Nepal): long-range atmospheric transport, glacier shrinkage, or local impact of tourism? Sci. Total Environ. 544, 382-390.

Jafarabadi, A.R., Bakhtiari, A.R., Aliabadian, M., Toosi, A.S., 2017. Spatial distribution and composition of aliphatic hydrocarbons, polycyclic aromatic hydrocarbons and hopanes in superficial sediments of the coral reefs of the Persian Gulf, Iran Environ. Pollut. 224, 159-223.

Jiang, Y.F., Yves, U.J., Sun, H., Hu, H.F., Zhan, H.Y., Wu, Y.Q., 2016. Distribution, compositional pattern and sources of polycyclic aromatic hydrocarbons in urban

soils of an industrial city, Lanzhou, China. Ecotoxicol. Environ. Saf. 126, 154-162.

Kannan, K., Johnson, B.R., Yohn, S.S., Giesy, J.P. Long, D.T., 2005. Spatial and temporal distribution of polycyclic aromatic hydrocarbons in sediments from inland lakes in Michigan, Environ. Sci. Technol. 39(13), 4700-4706.

Khairy, M.A., Luek, J.L., Dickhut, R., Lohmann, R., 2016. Levels, sources and chemical fate of persistent organic pollutants in the atmosphere and snow along the western Antarctic Peninsula. Environ. Pollut. 216, 304-313.

Khalili, N.R., Scheff, P.A. Holsen, T.M., 1995. PAH source fingerprints for coke ovens, diesel and gasoline engine highway tunnels and wood combustion emissions. Atmos. Environ. 29(4), 533-542.

Klerkx, J., Imanackunov, B., 2002. Lake Issyk-Kul: Its natural environment. Springer Netherlands, pp vii.

Kriegel, D., Mayer, C., Hagg, W., Vorogushyn, S., Duethmann, D., Gafurov, A., et al., 2013. Changes in glacierisation, climate and runoff in the second half of the 20th century in the Naryn basin, Central Asia. Glob. Planet. Chang. 110, 51-61.

Laflamme, R.E., Hites, R.A., 1978. The global distribution of polycyclic aromatic hydrocarbons in recent sediments. Geochim. Cosmochim. Ac. 42(3), 289-303.

Li, Q.Y., Wu, J.L., Sakiev, K., 2019. Organochlorine pesticides (OCPs) in soils near and around Lake Son-Kul in the western Tian Shan Mountains, Central Asia. J. Soils Sediment. 19 (4), 1685-1696.

Luo, W., Gao, J., Bi, X., Xu, L., Guo, J., Zhang, Q., 2016. Identification of sources of

polycyclic aromatic hydrocarbons based on concentrations in soils from two sides of the Himalayas between China and Nepal. Environ. Pollut. 212, 424-432.

Ma, J., Hung, H., Tian, C., Kallenborn, R., 2011. Revolatilization of persistent organic pollutants in the Arctic induced by climate change. Nat. Clim. Change. 1(5), 255-260.

Mamatkanov, D.M., Bajanova, L.V., Romanovskiy, V.V., 2006. Water resources of Kyrgyzstan in modern days. Ilim, Bishkek (in Russian).

Mathis, M., Sorrel, P., Klotz, S., Huang, X., Oberhänsli, H., 2014. Regional vegetation patterns at lake Son Kul reveal Holocene climatic variability in central Tien Shan (Kyrgyzstan, Central Asia). Quat Sci Rev 89, 169-185.

Miguel, A.H., Eiguren-Fernandez, A., Jaques, P.A., Froines, J.R., Grant, B.L., Mayo, P.R., et al., 2004. Seasonal variation of the particle size distribution of polycyclic aromatic hydrocarbons and of major aerosol species in Claremont, California. Atmos. Environ. 38, 3241-3251.

Mikkola, H., 2012. Implication of alien species introduction to loss of fish biodiversity and livelihoods on Issyk-Kul Lake in Kyrgyzstan, in: Biodiversity Enrichment in a Diverse World, edited by: Lameed, G. A., InTech Press, Rijeka, Croatia, ISBN-13: 978-953-51-0718-7, 395-419.

Norris, G., Duvall, R., Brown, S., Bai, S., 2014. EPA Positive Matrix Factorization (PMF) 5.0 Fundamentals and User Guide. Prepared for the US Environmental Protection Agency Office of Research and Development, Washington, DC. Inc., Petaluma.

Pacton, M., Sorrel, P., Bevillard, B., Zacaï, A., Vinçn-Laugier, A., Oberhänsli, H., 2015. Sedimentary facies analyses from nano- to millimetre scale exploring past microbial activity in a high-altitude lake (Lake Son Kul, Central Asia). Geol. Mag. 152(5), 902-922.

Pribylova, P., Kares, R., Boruvkova, J., Cupr, P., Prokes, R., Kohoutek, J., et al., 2012. Levels of persistent organic pollutants and polycyclic aromatic hydrocarbons in ambient air of Central and Eastern Europe. Atmos. Pollut. Res. 3(4), 494-505.

Ravindra, K., László, Bencs., Wauters, E., Hoog, J.D., Deutsch, F., Roekens, E., et al., 2006. Seasonal and site-specific variation in vapour and aerosol phase PAHs over Flanders (Belgium) and their relation with anthropogenic activities. Atmos. Environ. 40(4), 771-785.

Resmi, P., Manju, M., Gireeshkumar, T., Kumar, C.R., Chandramohanakumar, N., 2016. Source characterisation of Sedimentary organic matter in mangrove ecosystems of northern Kerala, India: Inferences from bulk characterisation and hydrocarbon biomarkers. Regional Stud. Mar. Sci. 7, 43-54.

Saba, B., Hashmi, I., Awan, M.A., Nasir, H., Khan, S.J., 2012. Distribution, toxicity level and concentration of polycyclic aromatic hydrocarbons (PAHs) in surface soil and groundwater of Rawalpindi, Pakistan. Desalin. Water Treat. 49(1-3), 240-247.

Schmid, M., 2011. Central Asia's Blue Pearl: The Issyk Kul Biosphere Reserve in Kyrgyzstan. Austrian MBA Committee (eds). In: Biosphere Reserves in the Mountains of the World. Excellence in the Clouds? Austrian Academy of Sciences

Press, Vienna, Austria, pp 73-76.

Shen, B.B., Wu, J.L., Zhao, Z.H., 2017. Organochlorine pesticides and polycyclic aromatic hydrocarbons in water and sediment of the Bosten Lake, Northwest China. J. Arid Land 9(2),287–298.

Shi, B., Wu, Q., Ouyang, H., Liu, X., Ma, B., Zuo, W., et al., 2014. Distribution and source apportionment of polycyclic aromatic hydrocarbons in soils and leaves from high-altitude mountains in Southwestern China. J. Environ. Qual. 43(6), 1942-1952.

Shirneshan, G., Bakhtiari, A.R., Memariani, M., 2017. Identifying the source of petroleum pollution in sediment cores of southwest of the Caspian sea using chemical fingerprinting of aliphatic and alicyclic hydrocarbons. Mar. Pollut. Bull. 115(1-2), 383-390.

Silva, T.S., Lopes, S.R.P., Spörl, G., Knoppers, B.A., Azevedo, D.A., 2012. Evaluation of anthropogenic inputs of hydrocarbons in sediment cores from a tropical Brazilian estuarine system. Microchem. J. 109,178-188.

Singh, D.P., Gadi, R., Mandal, T.K., 2012. Levels, sources, and toxic potential of polycyclic aromatic hydrocarbons in urban soil of Delhi, India. Hum. Ecol. Risk Assess. 18(2), 393-411.

Suman, S., Sinha, A., Tarafdar, A., 2016. Polycyclic aromatic hydrocarbons (PAHs) concentration levels, pattern, source identification and soil toxicity assessment in urban traffic soil of Dhanbad, India. Sci. Total Environ. 545-546(68), 353-360.

Tang, L., Tang, X., Zhu, Y., Zheng, M., Miao, Q., 2005. Contamination of polycyclic

aromatic hydrocarbons (PAHs) in urban soils in Beijing, China. Environ. Pollut. 31(6), 822-828.

Tremolada, P., Parolini, M., Binelli, A., Ballabio, C., Comolli, R., Provini, A., 2009. Preferential retention of POPs on the northern aspect of mountains. Environ. Pollut. 157(12), 3298-3307.

Tynybekov, A.K., Lelevkin, V.M., Kulenbekov, J.E., 2008. Environmental issues of the Kyrgyz Republic and Central Asia. In: Liotta PH (eds.), Environmental Change and Human Security: Recognizing and Acting on Hazard Impacts. Springer Netherlands, pp 407-432.

Vane, C. H., Kim, A.W., Beriro, D.J., Cave, M.R., Knights, K., Moss-Hayes, V., et al. 2014. Polycyclic aromatic hydrocarbons (PAH) and polychlorinated biphenyls (PCB) in urban soils of greater London, UK. Appl. Geochem. 51, 303-314.

Wang, C., Wu, S., Zhou, S., Wang, H., Li, B., Chen, H., et al., 2015. Polycyclic aromatic hydrocarbons in soils from urban to rural areas in Nanjing: Concentration, source, spatial distribution, and potential human health risk. Sci. Total Environ. 527-528, 375-383.

Wang, G.H, Mielke, W.H., Quach, V., Gonzales, C., Zhang, Q., 2004. Determination of polycyclic aromatic hydrocarbons and trace metals in New Orleans soils and sediments. Soil Sediment Contamin. 13, 313-327.

Wang, X.P., Yao, T.D., Cong, Z.Y., Yan, X.L., Kang, S.C., Zhang, Y., 2006. Gradient distribution of persistent organic contaminants along northern slope of central-Himalayas. China. Sci. Total Environ. 372, 193-202.

Wu, S., Liu, X., Liu, M., Chen, X., Liu, S., Cheng, L., et al. 2018. Sources, influencing factors and environmental indications of PAH pollution in urban soil columns of Shanghai, China. Ecol. Indic. 85, 1170-1180.

Wu, W.H., Wu, J.L., Song, F., Jilili, A., Saparov, A.S., Chen, X., et al. 2019. Spatial distribution and controlling factors of surface water stable isotope values (δ18O and δ2H) across Kazakhstan, Central Asia. Sci. Total Environ. 678, 53-61.

Yun, X., Yang, Y., Liu, M., Zhang, M., Wang, J., 2016. Distribution, seasonal variations, and ecological risk assessment of polycyclic aromatic hydrocarbons in the East Lake, China. CLEAN - Soil, Air Water 44, 506-514.

Yunker, M.B., Macdonald, R.W., Vingarzan, R., Mitchell, R.H., Goyette, D., Sylvestre, S., 2002. PAHs in the Fraser River basin: A critical appraisal of PAH ratios as indicators of PAH source and composition. Org. Geochem. 33, 489-515.

Zhang, Y., Su, Y., Liu, Z., Jeppesen, E., Yu, J., Jin, M., 2016. Geochemical records of anoxic water mass expansion in an oligotrophic alpine lake (Yunnan province, SW China) in response to climate warming since the 1980s. The Holocene 26(11), 1847-1857.

Zhang, Z.Y., Jilili, A., Jiang, F.Q., 2015. Heavy metal contamination, sources, and pollution assessment of surface water in the Tianshan Mountains of China. Environ. Monit. Assess. 187(2), 33.

Zhao, X., Kim, S.K., Zhu, W., Kannan, N., Li, D., 2015. Long-range atmospheric transport and the distribution of polycyclic aromatic hydrocarbons in Changbai mountain. Chemosphere 119, 289-294.

Zhao, Z.H., Zhang, L., Wu, J.L., 2016. Polycyclic aromatic hydrocarbons (PAHs) and organochlorine pesticides (OCPs) in sediments from lakes along the middle-lower reaches of the Yangtze River and the Huaihe River of China. Limnol. Oceanogr. 61(1), 47-60.

Zhao, Z.H., Zeng, H.A., Wu, J.L., Zhang, L., 2017. Concentrations, sources and potential ecological risks of polycyclic aromatic hydrocarbons in soils from Tajikistan. Int. J. Environ. Pollut. 61(1), 13-28.

Zhou, R., Yang, R., Jing, C., 2018. Polycyclic aromatic hydrocarbons in soils and lichen from the western Tibetan plateau: concentration profiles, distribution and its influencing factors. Ecotoxicol. Environ. Saf. 152, 151-158.

Supplementary material

Occurrence of polycyclic aromatic hydrocarbon (PAH) in soils around two typical lakes in the western Tian Shan Mountains (Kyrgyzstan, Central Asia): Local burden or global distillation?

Qianyu Li [a,c], Jinglu Wu [a,b,*], Jianchao Zhou [a], Kadyrbek Sakiev [d], Diana Hofmann [e]

[a] *State Key Laboratory of Lake Science and Environment Research, Nanjing Institute of Geography and Limnology, Chinese Academy of Sciences, Nanjing 210008, China*

[b] *Ecology and Environment of Central Asia, Chinese Academy of Sciences, Urumqi 830011, China*

[c] *University of Chinese Academy of Sciences, Beijing 100039, China*

[d] *Institute of Geology, National Academy of Sciences, Bishkek 720001, Kyrgyystan*

[e] *Institute of Bio- and Geosciences, IBG-3: Agrosphere, Forschungszentrum Jülich, Jülich 52425, Germany*

**Corresponding author:*

E-mail address: w.jinglu@niglas.ac.cn

Tel., +86-025-86882159

Chapters

Table contents

Figure contents

S1. Details for PAH diagnostic ratios

Ant/(Ant+Phe) is frequently used to distinguish between combustion and petrogenic/petroleum-related sources. A ratio of < 0.1 indicates petrogenic/petroleum-related sources, and a ratio of > 0.1 indicates a dominance of combustion (Bucheli et al., 2004). The ratio of Flt/(Flt+Pyr) is also used; that is, a Flt/(Flt+Pyr) ratio of < 0.4 indicates petrogenic/petroleum sources; a Flt/(Flt+Pyr) ratio in the range of 0.4–0.5 indicates petroleum combustion; and a Flt/(Flt+Pyr) ratio of > 0.5 indicates the combustion of domestic coal, grass, and wood (Bortey-Sam et al., 2014). The ratio of IP/(IP+BghiP) is similar to that of Flt/(Flt+Pyr). Moreover, the less promising molecular ratio of BaP/BghiP can be used to distinguish traffic (> 0.6) and non-traffic sources (< 0.6). Due to the overlap of characteristic PAH profiles from each source on the one hand and the selective decay of more labile compounds on the other side, the combination of two or more diagnostic ratios helps to provide a better estimation of PAH sources (Yunker et al., 2002).

S2. Limitation and details for positive matrix factorization (PMF)

The PMF analysis used PAH concentrations as input data and was run in robust mode (Norris et al., 2014). We categorized NAP as “bad” during operations in all kinds of functional areas due to its unstable nature. Besides, BghiP in P was categorized as “weak” because of lower correlation between the simulated and observed concentration. All other species showed signal-to-noise ratio (S/N) larger than three and were categorized as “strong” according to their good fitting results. After testing different number of factors (varied from 3 to 7) with random seed mode,

3 or 4, respectively were selected in terms of good fitting results and reasonable interpretation. One hundred-time run was set to make the fittings converged. The fitting results showed that all the residuals were at the range of ± 2, all the r^2 values were higher than 0.834 and most of the slope approached to 1, indicating the reliability of the simulation results.

S3. Description on *n*-alkanes for source apportionment

Carbon preference index (CPI), defined as the odd to even carbon-number n-alkanes values, is calculated by a value of 1 or close to 1 for the presence of n-alkanes from petroleum and anthropogenic activities (Silva et al., 2012). Unresolved complex mixture (UCM) is also an effective indicator to assess petroleum contamination from anthropogenic sources (Frysinger et al., 2003), especially pertinent to unburned petroleum emissions from vehicular traffic (Simoneit, 1989). Pristane (Pr, C_{19} isoprenoid) and Phytane (Ph, C_{20} isoprenoid) are among the most abundant isoprenoids in petroleum. While Ph originates only from petroleum hydrocarbons, Pr is also predominant in coal-related products (Volkman et al., 1992; Yunker et al., 2012). Therefore, Pr/Ph ratios more than 4 are typically for coal combustion, whereas values close to or lower than 1 indicate a petroleum origin (Medeiros et al., 2005).

Table S1. TOC contents and detailed information on sampling sites

Sampling sites	Latitude (º)	Longitude (º)	Altitude (m)	TOC (%)
S1	41.91626	75.06680	3022	4.09
S2	41.93322	75.11187	3034	6.41
S3	41.92196	75.15738	3024	2.97
S4	41.92469	75.19631	3063	5.43
S5	41.85875	75.33480	3054	2.48
S6	41.84020	75.37653	3050	3.72
S7	41.76232	75.37484	3019	4.03
S8	41.76744	75.28110	3040	4.55
S9	41.76124	75.13252	3019	4.34
S10	41.76735	75.07867	3019	0.71
S11	41.81082	75.04635	3017	6.72
S12	41.75253	75.04213	2850	4.76
S13	41.70257	75.03802	2750	8.10
S14	41.65921	75.01864	2689	1.24
S15	41.57751	75.02428	2124	2.24
S16	41.42879	75.03296	1703	0.31
S17	41.37448	75.62051	1838	1.27
S18	41.42871	75.68536	1876	0.36
S19	41.43141	75.95148	2520	1.06
S20	41.46105	76.22453	2117	0.80
S21	41.49609	76.42292	2032	1.03
S22	41.57224	75.86888	2150	1.06
S23	41.74432	75.72026	2263	4.14
Y1	42.31565	76.29405	1597	1.34
Y2	42.31813	76.39431	1656	1.07
Y3	42.19232	76.67874	1685	0.82
Y4	42.17377	77.39471	1623	0.88
Y5	42.15496	77.52770	1611	3.77
Y6	42.14858	77.59703	1996	0.42
Y7	42.01077	77.61351	1775	4.22
Y8	42.34613	78.01371	1754	2.22
Y9	42.48405	78.38149	1746	4.47
Y10	42.59319	78.38597	1619	0.92
Y11	42.73868	78.34640	1612	2.35
Y12	42.75067	78.12400	1590	9.97
Y13	42.83453	77.50374	2105	10.73
Y14	42.49803	76.48075	1604	3.08
Y15	42.72438	78.92904	2151	2.94
Y16	42.74728	78.96597	1957	2.04

Table S2. Recoveries for the 16 priority PAHs.

PAHs congeners	Abbreviations	Number of rings	Matrix-based recoveries (%)
naphthalene	Nap	2	72.1
acenaphthylene	Acy	3	82.5
acenaphthene	Ace	3	76.4
fluorene	Flu	3	86.3
phenanthrene	Phe	3	83.1
anthracene	Ant	3	81.8
fluoranthene	Flt	4	90.6
pyrene	Pyr	4	78.4
benzo[*a*]anthracene	BaA	4	84.3
chrysene	Chr	4	88.1
benzo[*b*]fluoranthene	BbF	5	80.6
benzo[*k*]fluoranthene	BkF	5	92.2
benzo[*a*]pyrene	BaP	5	93.4
dibenzo[*a,h*]anthracene	DahA	5	104.8
benzo[*g,h,i*]perylene	BghiP	6	97.6
indeno[1,2,3-cd]pyrene	IP	6	89.7

Table S3. Regional comparison of total PAH concentrations in this study with other similar areas (ng/g dw).

Clusters	Locations	∑16 PAHs (ng/g dw)	Dominated rings	References
Industrial and urban regions	Group 1	947-9439 (4760±3525)	4-,5- and 3- rings	This study
	Shanghai, China	153-15221 (2372±1839)	4-,5- and 6- rings	Wu et al., 2018
	Kathmandu and Pokhara, Nepal	17-6219 (1172)	-	Pokhrel et al., 2018
	Kocaeli, Turkey	49-10512 (992 ± 1323)	4-,5- and 6- rings	Cetin et al., 2017
	Erbil metropolis, Iraq	24.3-6129.14 (2296)	4- and 5-rings	Amjadian et al., 2016
	Lanzhou, China	391-10900 (2240)	4-ring	Jiang et al., 2016
	Dhanbad, India	1019-10856 (3488)	4- and 5-rings	Suman et al., 2016
	the Northern Czech Republic	153-336169 (8022±33988)	-	Vácha et al., 2015
	London, UK	4000-67000 (18000)	4-,5- and 6- rings	Vane et al., 2014
	Rawalpindi, Pakistan	2700-4443 (3672 ± 592)	3- and 4-rings	Saba et al., 2012
	Delhi, India	11460 ± 8390	4- and 5-rings	Singh et al., 2012
	Detroit, USA	7843	4-,5- and 6- rings	Wang et al., 2008
	Boston, USA	~ -360000 (19000)	4-,5- and 6- rings	Wang et al., 2004
Agricultural and rural regions	Group 2	150-1287 (481±374)	3- and 4-rings	This study
	Lebanon			Soukarieh et al., 2018
	Shanghai, China	223-8214 (1552)	2-,3- and 4-rings	Tong et al., 2018
	Nanjing, China	24.3-9310 (1680)	4- and 5-rings	Wang et al., 2015
	Central Europe	872-7350 (4300±2770)	-	Bosch et al., 2015
	Ulsan, Korea	92-450 (220)	2- and 3-rings	Kwon and Choi, 2014
	Delhi, India	1550 ± 1070	2- and 3-rings	Singh et al., 2012
	South Korea	23.3-2834 (236)	3- and 4-rings	Nam et al., 2003
Mountain regions	Group 3	51.9-299 (136±75)	3- and 4-rings	This study
	Western Tibetan Plateau, China	14.4-59.5 (30.8)	2- and 3-rings	Zhou et al., 2018
	Mountains in Tajikistan	17.2-258 (66.3±58.2)	3- and 4-rings	Zhao et al., 2017
	the Southern side of the Himalayas	15.3-4762 (458)	4- and 5-rings	Devi et al., 2016
	the Northern side of the Himalayas	2.30-327 (126)	2- and 3-rings	Luo et al., 2016
	Kongsfjorden, Norway	12-2315 (139)	3- and 4-rings	Szczybelski et al., 2016
	Changbai Mountain, China	38.5-443	3- and 4-rings	Zhao et al., 2015
	Mountains in Southwestern China	93.9-802 (252)	2- and 3-rings	Shi et al., 2014
	Pyrenees Mountains, Spain	420±100	-	Quiroz et al., 2011
	Mountains in western Canada	2.00-789 (167)	2- and 3-rings	Choi et al., 2009
	Italy Alps	6.00-80.0 (20.0)	3- and 4-rings	Tremolada et al., 2009

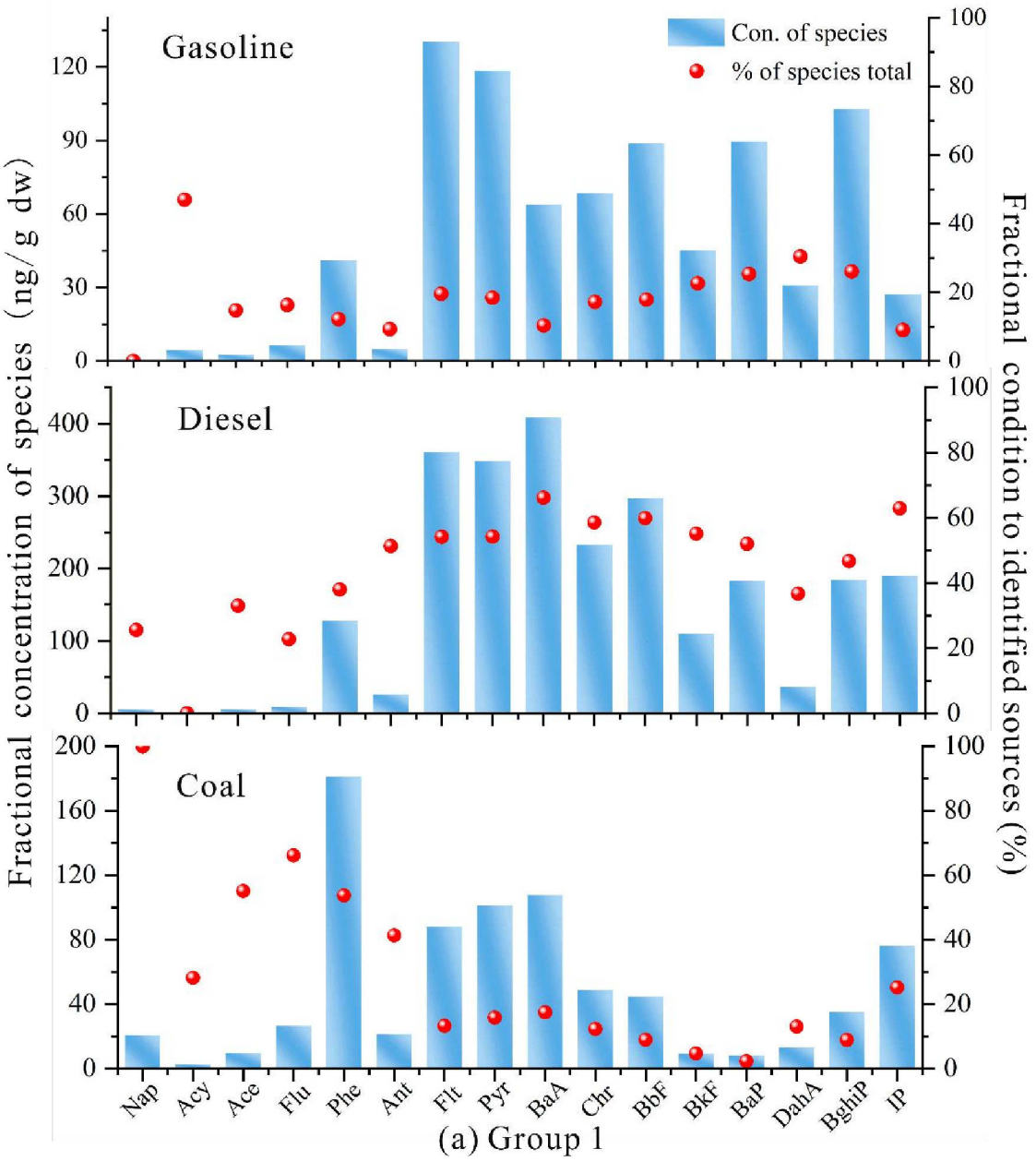
Gasoline
Diesel
Coal
Con. of species
% of species total
Fractional concentration of species (ng/g dw)
Fractional condition to identified sources (%)
Nap
Acy
Ace
Flu
Phe
Ant
Flt
Pyr
BaA
Chr
BbF
BkF
BaP
DahA
BghiP
IP

(a) Group 1

1

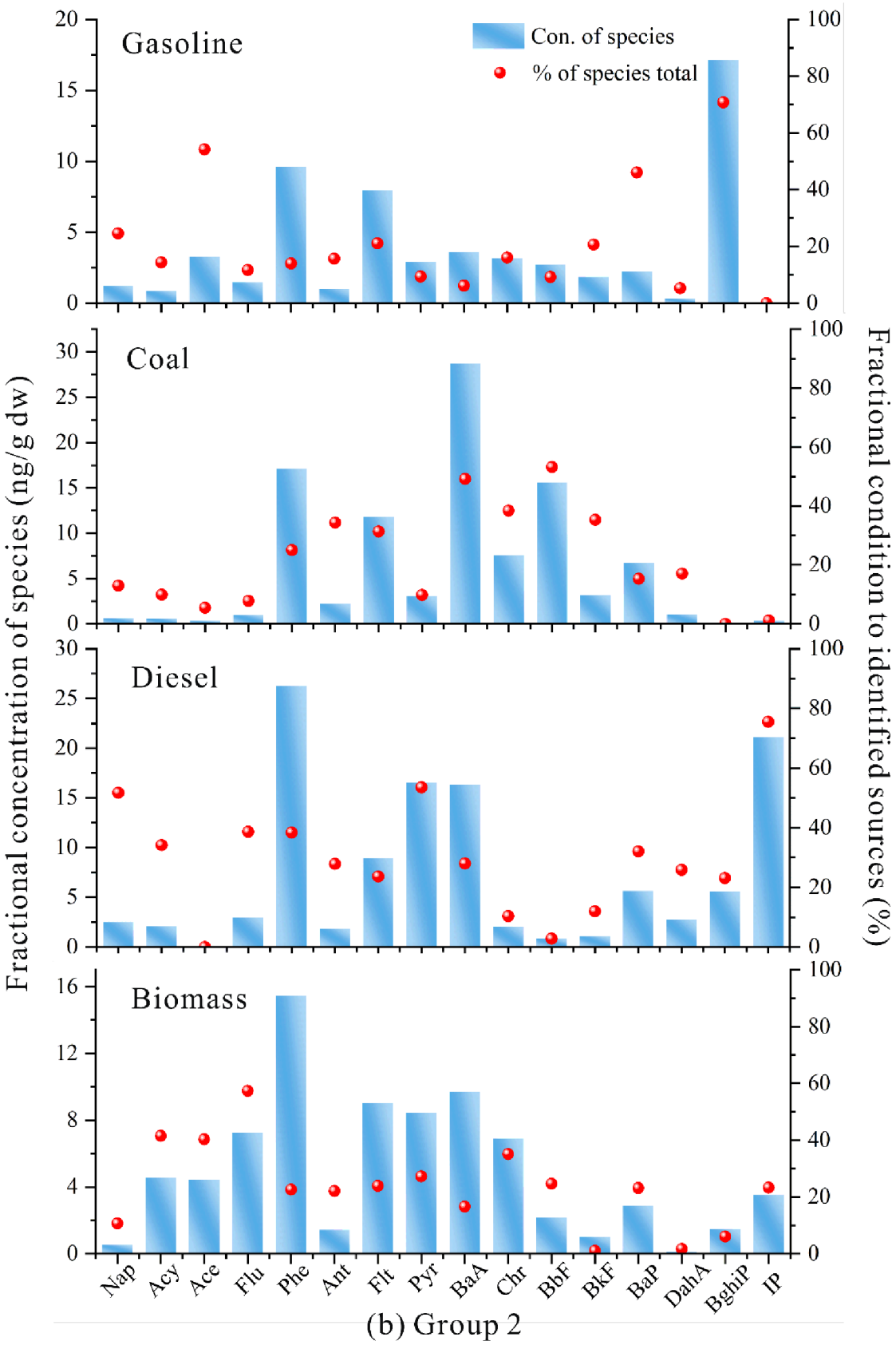
Gasoline
Coal
Diesel
Biomass
Con. of species
% of species total
Fractional concentration of species (ng/g dw)
Fractional condition to identified sources (%)
Nap
Acy
Ace
Flu
Phe
Ant
Flt
Pyr
BaA
Chr
BbF
BkF
BaP
DahA
BghiP
IP

(b) Group 2

2

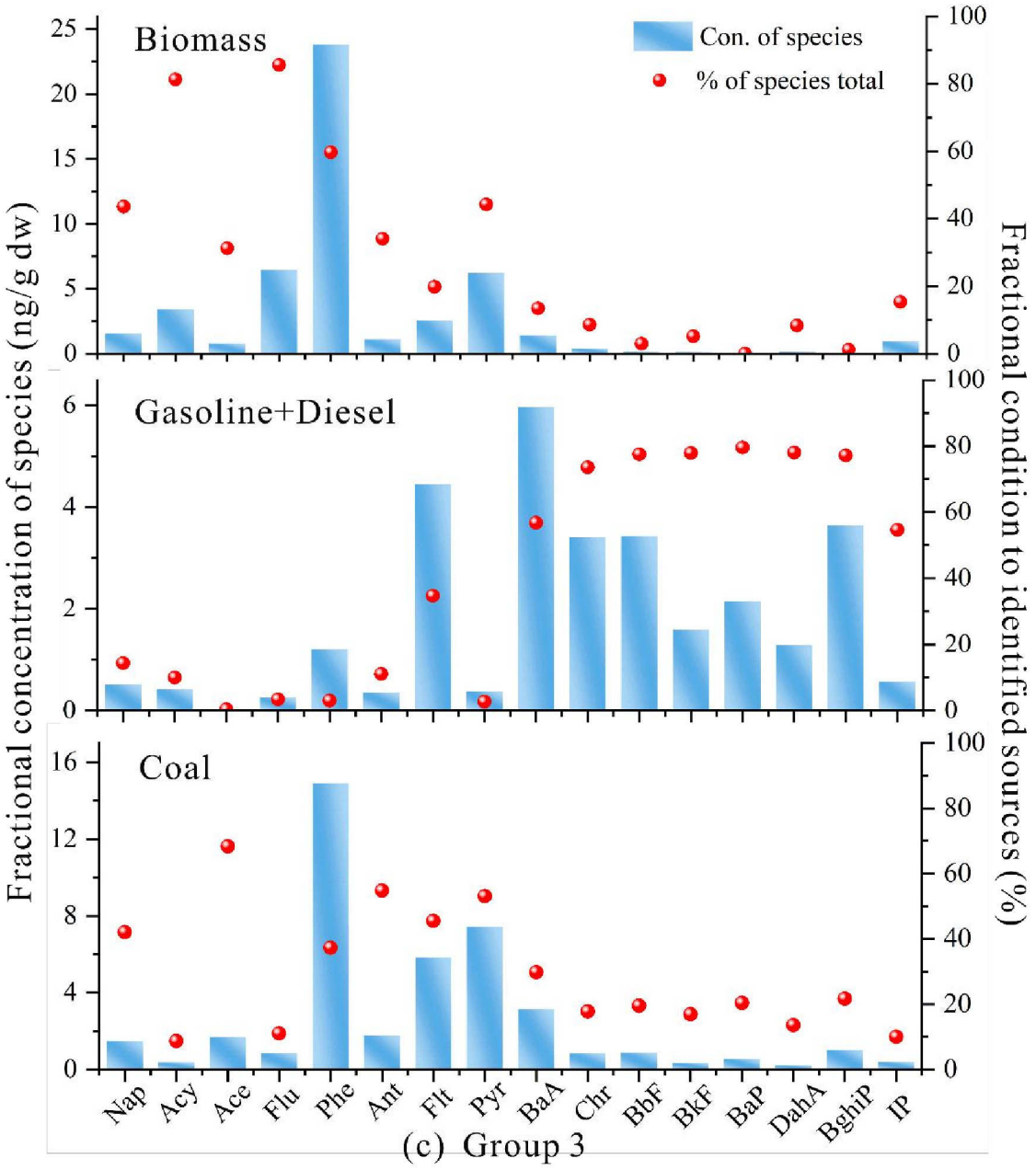

Fig. S1. Source profiles obtained from the PMF model of (a) Group 1, (b) Group 2, and (c) Group 3, respectively.

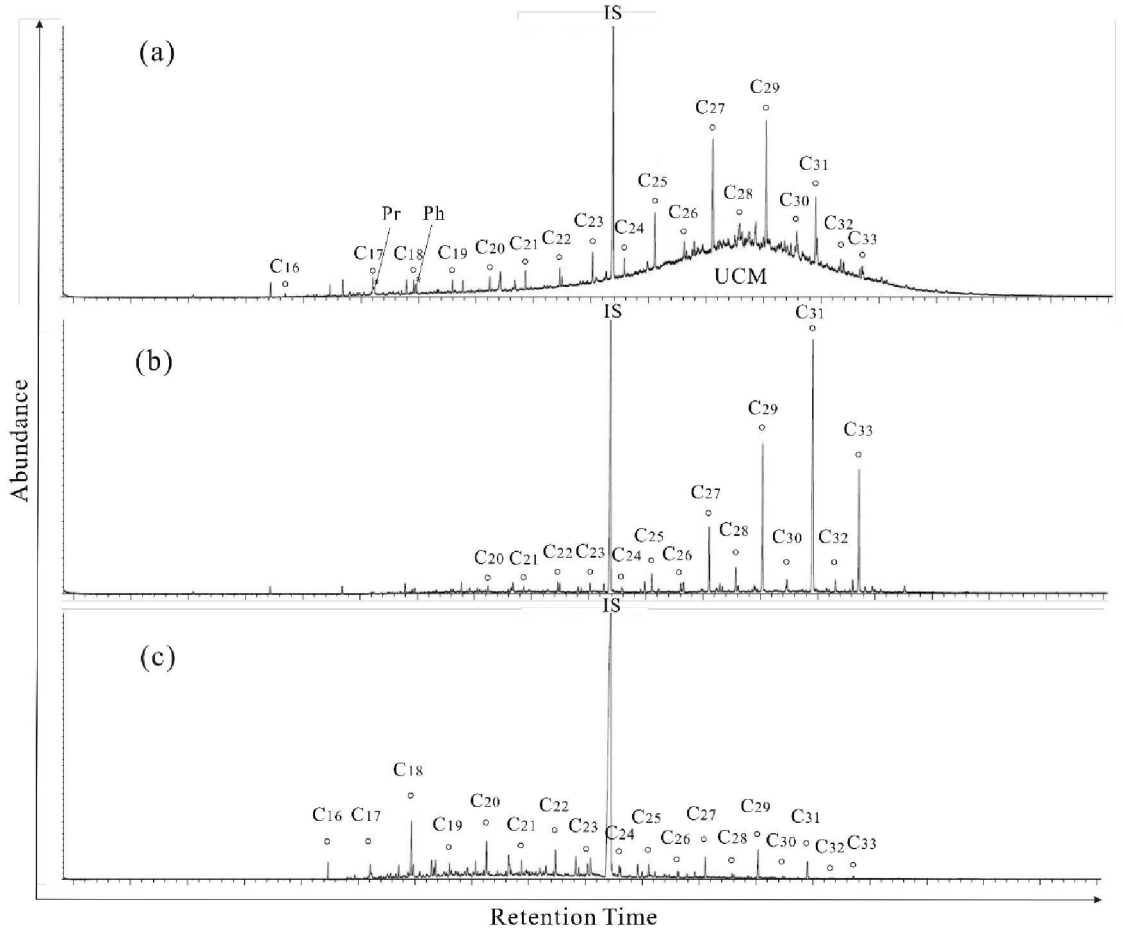

Fig. S2. GC–MS chromatograms of distribution patterns of individual *n*-alkanes in soils from the study area. (a) unimodal distribution of *n*-alkanes with unresolved complex mixture (UCM) observed in Group 1 and Group 2; (b) unimodal distribution of *n*-alkanes observed in Group 3; (c) bimodal distribution of *n*-alkanes observed in Group 3.

References

Amjadian, K., Sacchi, E., Mehr, M.R., 2016. Heavy metals (HMs) and polycyclic aromatic hydrocarbons (PAHs) in soils of different land uses in Erbil metropolis, Kurdistan region, Iraq. Environ. Monit. Assess. 188(11), 605.

Bortey-Sam, N., Ikenaka, Y., Nakayama, S.M., Akoto, O., Yohannes, Y.B., Baidoo, E., et al., 2014. Occurrence, distribution, sources and toxic potential of polycyclic aromatic hydrocarbons (PAHs) in surface soils from the Kumasi metropolis, Ghana. Sci. Total Environ. 496, 471-478.

Bosch, C., Andersson, A., Kruså, M., Bandh, C., Hovorková, I., Klánová, J., et al. 2015. Source apportionment of polycyclic aromatic hydrocarbons in Central European soils with compound-specific triple isotopes ($\delta^{13}C$, $\delta^{14}C$, and $\delta^{2}H$). Environ. Sci. Technol. 49(13), 7657-7665.

Bucheli, T.D., Blum, F., Desaules, A., Gustafsson, O., 2004. Polycyclic aromatic hydrocarbons, black carbon, and molecular markers in soils of Switzerland, Chemosphere 56(11), 1061-1076.

Cetin, B., Yurdakul, S., Keles, M., Celik, I., Ozturk, F., Dogan, C., 2017. Atmospheric concentrations, distributions and air-soil exchange tendencies of PAHs and PCBs in a heavily industrialized area in Kocaeli, Turkey. Chemosphere 183, 69-79.

Choi, S.D., Shunthirasingham, C., Daly, G.L., Xiao, H., Lei, Y.D., Wania, F., 2009. Levels of polycyclic aromatic hydrocarbons in Canadian mountain air and soil are

controlled by proximity to roads. Environ. Pollut. 157(12), 3199-3206.

Devi, N.L., Yadav, I.C., Qi, S.H., Yang, D., Gan, Z., Raha, P., 2016. Environmental carcinogenic polycyclic aromatic hydrocarbons in soil from Himalayas, India: implications for spatial distribution, sources apportionment and risk assessment. Chemosphere 144, 493-502.

Frysinger, G.S., Gaines, R.B., Xu, L., Reddy, C.M., 2003. Resolving the unresolved complex mixture in petroleum-contaminated sediments. Environ. Sci. Technol. 37, 1653-1662.

Jiang, Y.F., Yves, U.J., Sun, H., Hu, X.F., Zhan, H.Y., Wu, Y.Q., 2016. Distribution, compositional pattern and sources of polycyclic aromatic hydrocarbons in urban soils of an industrial city, Lanzhou, China. Ecotoxicol. Environ. Saf. 126, 154-162.

Kwon, H.O., Choi, S.D., 2014. Polycyclic aromatic hydrocarbons (PAHs) in soils from a multi-industrial city, South Korea. Sci. Total Environ. 470-471, 1494-1501.

Luo, W., Gao, J., Bi, X., Xu, L., Guo, J., Zhang, Q., 2016. Identification of sources of polycyclic aromatic hydrocarbons based on concentrations in soils from two sides of the Himalayas between China and Nepal. Environ. Pollut. 212, 424-432.

Medeiros, P.M., Bicego, M.C., Castelao, R.M., Del Rosso, C., Fillmann, G., Zamboni, A.J., 2005. Natural and anthropogenic hydrocarbon inputs to sediments of Patos Lagoon Estuary, Brazil. Environ. Int. 31(1), 77-87.

Nam, J.J., Song, B.H., Eom, K.C., Lee, S.H., Smith, A., 2003. Distribution of polycyclic aromatic hydrocarbons in agricultural soils in South Korea.

Chemosphere 50(10), 1281-1289.

Pokhrel, B., Gong, P., Wang, X., Chen, M., Gao, S., 2018. Distribution, sources, and air–soil exchange of OCPs, PCBs and PAHs in urban soils of Nepal. Chemosphere 200, 532-541.

Quiroz, R., Grimalt, J.O., Fernandez, P., Camarero, L., Catalan, J., Stuchlik, E., et al. 2011. Polycyclic aromatic hydrocarbons in soils from European high mountain areas. Water Air Soil Pollut. 215(1-4), 655-666.

Saba, B., Hashmi, I., Awan, M.A., Nasir, H., Khan, S.J., 2012. Distribution, toxicity level and concentration of polycyclic aromatic hydrocarbons (PAHs) in surface soil and groundwater of Rawalpindi, Pakistan. Desalin. Water Treat. 49(1-3), 240-247.

Shi, B., Wu, Q., Ouyang, H., Liu, X., Ma, B., Zuo, W., et al., 2014. Distribution and source apportionment of polycyclic aromatic hydrocarbons in soils and leaves from high-altitude mountains in Southwestern China. J. Environ. Qual. 43(6), 1942-1952.

Simoneit, B.R., 1989. Organic matter of the troposphere — V: Application of molecular marker analysis to biogenic emissions into the troposphere for source reconciliations. J. Atmos. Chem. 8, 251-275.

Singh, D.P., Gadi, R., Mandal, T.K., 2012. Levels, sources, and toxic potential of polycyclic aromatic hydrocarbons in urban soil of Delhi, India. Hum. Ecol. Risk Assess. 18(2), 393-411.

Soukarieh, B., El Hawari, K., El Husseini, M., Helene, Budzinski, H., Jaber, F., 2018.

77 Impact of Lebanese practices in industry, agriculture and urbanization on soil
78 toxicity. Evaluation of the Polycyclic Aaromatic Hydrocarbons (PAHs) levels in
79 soil. Chemosphere 210, 85-92.
80 Suman, S., Sinha, A., Tarafdar, A., 2016. Polycyclic aromatic hydrocarbons (PAHs)
81 concentration levels, pattern, source identification and soil toxicity assessment in
82 urban traffic soil of Dhanbad, India. Sci. Total Environ. 545-546(68), 353-360.
83 Szczybelski, A.S., van den Heuvel-Greve, M.J., Kampen, T., Wang, C., van den Brink,
84 N.W., Koelmans, A.A., 2016. Bioaccumulation of polycyclic aromatic
85 hydrocarbons, polychlorinated biphenyls and hexachlorobenzene by three Arctic
86 benthic species from Kongsfjorden (Svalbard, Norway). Mar. Pollu. Bull. 112,
87 65-74.
88 Tong, R., Yang, X., Su, H., Pan, Y., Zhang, Q., Wang, J., et al., 2018. Levels, sources
89 and probabilistic health risks of polycyclic aromatic hydrocarbons in the
90 agricultural soils from sites neighboring suburban industries in Shanghai. Sci.
91 Total Environ. 616-617, 1365-1373.
92 Tremolada, P., Parolini, M., Binelli, A., Ballabio, C., Comolli, R., Provini, A., 2009.
93 Preferential retention of POPs on the northern aspect of mountains. Environ.
94 Pollut. 157(12), 3298-3307.
95 Vane, C. H., Kim, A.W., Beriro, D.J., Cave, M.R., Knights, K., Moss-Hayes, V., et al.
96 2014. Polycyclic aromatic hydrocarbons (PAH) and polychlorinated biphenyls
97 (PCB) in urban soils of greater London, UK. Appl. Geochem. 51, 303-314.
98 Vácha, R., Skála, J., Čechmánková, J., Horváthová, V., Hladík, J., 2015. Toxic

elements and persistent organic pollutants derived from industrial emissions in agricultural soils of the Northern Czech Republic. J. Soils Sediments 15(8), 1813-1824.

Volkman, J.K., Holdsworth, D.G., Neill, G.P., Bavor, H.J.Jr., 1992. Identification of änatural, anthropogenic and petroleum hydrocarbons in aquatic sediments. Sci. Total Environ. 112, 203-219.

Wang, C., Zhou, S., Song, J., Wu, S., 2017. Human health risks of polycyclic aromatic hydrocarbons in the urban soils of Nanjing, China. Sci. Total Environ. 612, 750-757.

Wang, G., Zhang, Q., Ma, P., Rowden, J., Mielke, H.W., Gonzales, C., et al., 2008. Sources and distribution of polycyclic aromatic hydrocarbons in urban soils: Case studies of Detroit and New Orleans. Soil Sediment Contamin. 17(6), 547-563.

Wang, G.H, Mielke, W.H., Quach, V., Gonzales, C., Zhang, Q., 2004. Determination of polycyclic aromatic hydrocarbons and trace metals in New Orleans soils and sediments. Soil Sediment Contamin. 13, 313-327.

Wu, S., Liu, X., Liu, M., Chen, X., Liu, S., Cheng, L., et al., 2018. Sources, influencing factors and environmental indications of PAH pollution in urban soil columns of Shanghai, China. Ecol. Indic. 85, 1170-1180.

Yunker, M.B., Macdonald, R.W., Vingarzan, R., Mitchell, R.H., Goyette, D., Sylvestre, S., 2002. PAHs in the Fraser River basin: A critical appraisal of PAH ratios as indicators of PAH source and composition. Org. Geochem. 33, 489-515.

Yunker, M.B., Perreault, A., Lowe, C.J., 2012. Source apportionment of elevated PAH

concentrations in sediments near deep marine outfalls in Esquimalt and Victoria, BC, Canada: Is coal from an 1891 shipwreck the source? Org. Geochem. 46, 12-37.

Zhao, X., Kim, S.K., Zhu, W., Kannan, N., Li, D., 2015. Long-range atmospheric transport and the distribution of polycyclic aromatic hydrocarbons in Changbai mountain. Chemosphere 119, 289-294.

Zhao, Z.H., Zeng, H.A., Wu, J.L., Zhang, L., 2017. Concentrations, sources and potential ecological risks of polycyclic aromatic hydrocarbons in soils from Tajikistan. Int. J. Environ. Pollut. 61(1), 13-28.

Zhou, R., Yang, R., Jing, C., 2018. Polycyclic aromatic hydrocarbons in soils and lichen from the western Tibetan plateau: concentration profiles, distribution and its influencing factors. Ecotoxicol. Environ. Saf. 152, 151-158.